A THESIS SUBMITTED TO
THE GRADUATE SCHOOL OF NATURAL AND APPLIED SCIENCES
OF ÇANKIRI KARATEKİN UNIVERSITY

SOLVING HIGHER ORDER PARTIAL DIFFERENTIAL EQUATIONS USING MESH FREE METHOD

IN PARTIAL FULFILLMENT OF THE REQUIREMENTS
FOR
THE DEGREE OF MASTER OF SCIENCE
IN
MATHEMATICAL SCIENCE

BY

MOHAMMED ABDULRASOOL HASAN AL-DULAIMI

ÇANKIRI

2023

SOLVING HIGHER ORDER PARTIAL DIFFERENTIAL EQUATIONS USING MESH FREE METHOD

By Mohammed Abdulrasool Hasan AL-DULAIMI

June 2023

We certify that we have read this thesis and that in our opinion it is fully adequate, in scope and in quality, as a thesis for the degree of Master of Science

Advisor : Asst. Prof. Dr. Şerifenur CEBESOY ERDAL
Co-Advisor : Asst. Prof. Dr. Saad Qasim Abbas ALBEATY

Examining Committee Members:

Chairman : Assoc. Prof. Dr. Tuğba YURDAKADİM
Mathematics
Bilecik Şeyh Edebali University

Member : Asst. Prof. Dr. Şerifenur CEBESOY ERDAL
Mathematics
Çankırı Karatekin University

Member : Asst. Prof. Dr. Celalettin KAYA
Mathematics
Çankırı Karatekin University

Approved for the Graduate School of Natural and Applied Sciences

Prof. Dr. Hamit ALYAR
Director of Graduate School

I hereby declare that all information in this document has been obtained and presented in accordance with academic rules and ethical conduct. I also declare that, as required by these rules and conduct, I have fully cited and referenced all material and results that are not original to this work.

Mohammed Abdulrasool Hasan AL-DULAIMI

ABSTRACT

SOLVING HIGHER ORDER PARTIAL DIFFERENTIAL EQUATIONS USING MESH FREE METHOD

Mohammed Abdulrasool Hasan AL-DULAIMI

Master of Science in Mathematics

Advisor: Asst. Prof. Dr. Şerifenur CEBESOY ERDAL

Co-Advisor: Asst. Prof. Dr. Saad Qasim Abbas ALBEATY

June 2023

In this work, a novel numerical mesh-free method is offered to solve time-dependent issues with changing parameter controlled via higher types of partial differential equations. This method is more suitable than normal diffusion formulas for defining response propagation for such research disciplines. To cope with both the time variable as well as its derivatives, the finite differences approach is used and the radial basis functions technique is created for diffusion equation. To verify the correctness of our approach, numerical experimentation results are provided and contrasted with analytic results.

2023, 44 pages

Keywords: Higher order partial differential equations, Finite element, Meshfree, Weak solution

ÖZET

AĞSIZ YÖNTEMLER KULLANARAK YÜKSEK BASAMAKTAN KISMİ DİFERENSİYEL DENKLEMLERİN ÇÖZÜLMESİ

Mohammed Abdulrasool Hasan AL-DULAIMI
Matematik, Yüksek Lisans
Tez Danışmanı: Dr. Öğr. Üyesi Şerifenur CEBESOY ERDAL
Eş Danışman: Dr. Saad Qasim Abbas ALBEATY
Haziran 2023

Bu çalışmada, daha yüksek türde kısmi diferensiyel denklemler aracılığıyla kontrol edilen değişen parametre ile zamana bağlı sorunları çözmek için yeni bir sayısal ağsız yöntem sunulmuştur. Bu yöntem, bu tür araştırma disiplinleri için yanıt yayılımını tanımlamak adına normal yayılma formüllerinden daha uygundur. Hem zaman değişkeni hem de türevleri ile başa çıkmak için sonlu farklar yaklaşımı kullanılmış ve difüzyon denklemi için radyal tabanlı fonksiyonlar tekniği oluşturulmuştur. Yaklaşımımızın doğruluğunu doğrulamak için sayısal deney sonuçları verilmiş ve analitik sonuçlarla karşılaştırılmıştır.

2023, 44 sayfa

Anahtar Kelimeler: Yüksek mertebeden kısmi diferensiyel denklemler, Sonlu eleman, Meshfree, Zayıf çözüm.

PREFACE AND ACKNOWLEDGEMENTS

First of all, my deep thanks and gratitude are presented to almighty ALLAH (Glorified and exalted He be) for my success and inspiration in gaining this great opportunity to develop my professional life. The greatest thanks for Ministry of Education and Turkish Government for giving me the chance to get the Master degree from ÇANKIRI KARATEKİN UNIVERSITY.

I would like to thank my thesis advisor, **Asst. Prof. Dr. Şerifenur CEBESOY ERDAL**, for his patience, guidance and understanding.

I would like to express my thanks and gratitude to my secondary advisor, **Asst. Prof. Dr**. **Saad Qasim Abbas ALBEATY**, for his assistance and advice throughout the entire dissertation.

I would also like to thank my family for their support and encouragement. Finally I would like to express my thanks to everyone who helped me complete this thesis.

Mohammed Abdulrasool Hasan AL-DULAIMI
Çankırı-2023

CONTENTS

LIST OF SYMBOLS

u'(x)	Derivative of u
Δ	Laplace operation
ℓ	Linear partial differential operation
ζ and ϕ	Radial kernel function
$u_{xx}(x,t)$	Second partial derivative of u
$H_0^2(\phi;\mathrm{R})$	Sobolev space
$\Re_j^i$	Space of *i*- change polynomial of order not exceed *j*
L^2	The second norm

LIST OF ABBREVIATIONS

DEs	Differential equations
FDM	Finite difference method
ODEs	Ordinary differential equations
PDEs	Partial differential equations
RKFs	Radical kernel functions
RMQ	Reverse multiquadric
RMS	Root mean square
SFS	Splines flat sheets

LIST OF FIGURES

LIST OF TABLES

1. INTRODUCTION

Most physical models use higher-order and nonlinear partial differential equation (PDEs). Since they contain fourth-order spatial derivative elements, the PDEs regulating Kirchhoff-Love plates and thin shells, for instance, are higher-order (Reddy 2006). The biharmonic part in the Cahn-Hilliard phase-field formula, that describes the spontaneously dissociation of a bisexual fluid's components, is likewise of fourth order (Cahn *et al.* 1996). Nonlinear PDEs can appear in any research of inelasticity due to material flexibility and significant displacement, for instance, see Simo and Hughes 1985. To solve the PDEs that arise in these situations, scientists require trustworthy numerical techniques.

In order to solve the class of higher-order partial differential equations' specified technical and mathematical issues, high-order numerical techniques are frequently applied. They are utilized, among several other things, in the modelling of hydromagnetic, astronomy, burning thermal stability and acoustic waves. In fluid mechanics, higher-order derivatives, such as those of the fifth or eighth orders, are being used to add fake stiffness factors or to approximation filtering effects (Kajishima and Taira 2016).

In these issues, an accurate calculation of the higher-order derivatives necessitates the use of complex and very precise techniques; alternatively, the generated mistakes operate as artificially added terms that compromise the precision of a result. In a review study, Boutayeb and Chetouani introduced and discussed numerous numerical techniques utilized for higher-order derivative partitioning (Boutayeb and Chetouani 2007).

The finite element approach is mostly used in computer investigations of higher-order and nonlinear partial differential equations in mechanics. The finite element approach has drawbacks relating to lattice dependence and issues brought on by the usage of the weak version, especially when used to higher-order and nonlinear PDEs in physics. For instance, the numerical solution should be broken down into systems of lower-order PDEs in order to utilize the finite element approach for higher-order PDEs. Higher-order quadratic shapes and global continuation of the numerical solution are required for finite element approach implementation of the associated weak shapes, which increases computing cost (Beel *et al.* 2019).

The finite element approach domains integrating with conventional quadrature methods becomes challenging in nonlinear situations involving physical or contacting surfaces or other irregularities, and particular adjustments should be performed to address these challenges (Yoon and Song 2014). To avoid the likelihood of component node-to-segment contacting, specific approaches must be devised, especially for contact issues.

To address several of the issues with the finite element approach, weak form-based meshfree techniques have been developed, like the component Galerkin method (Belytschko *et al.* 1994). In (Rabczuk and Belytschko 2004, Rabczuk *et al.* 2004, Anitescu *et al.* 2015) include other intriguing weak form-based meshfree approaches. Even though these techniques do away with mesh dependence, they still need area integration and precise derivative computing, which raises computational costs. Given these challenges, it seems sense to investigate further numerical techniques for resolving higher-order PDS.

2. LITERATURE REVIEW

The study focuses on the numerical calculation of the nonhomogeneous time-dependent issue with the governing equations as follows:

$$\frac{\partial u^{(n)}}{\partial t} + \lambda_{n-1}\beta \frac{\partial u^{(n-1)}}{\partial t} + \cdots + \lambda_1 \beta \frac{\partial u}{\partial t} + \lambda_0 = \xi_{n-1} g_{n-1}(x) \frac{\partial u^{(n-1)}}{\partial x} + \cdots + \xi_1 g_1(x) + \kappa\beta u + g_2(x,t),$$

where $\lambda_{n-1}, \ldots, \lambda_1, \xi_{n-1}, \ldots, \xi_1$, and κ are constants, g_{n-1}, $g_1(x)$ and $g_2(x,t)$ are provided analytic functions, and $\beta \in \{0,1\}$. The telegraph issue and the waves issue, accordingly, are represented by the situations where $\beta = 0$ and $\beta = 1$.

The spreading of electromagnetic waves in conductors media, the planar random motion of an electron in liquid dynamics, the transmission of electrical desires in the nerve fibers of muscles and nerve cells, and the spreading of shock wave resulting from inspiratory blood circulation in airways are all described by electrostatic formulas. Another crucial second-order linear PDEs for such representation of waves, including voice, sight, and standing waves, is the ripple formula. It occurs in disciplines including hydrodynamics, electrochemistry, and acoustical.

Numerous numerical techniques, including as the finite elements, and interpolation approaches, have already been created during the recent decades to handle bounding issues involving ordinary and partial differential equations. Finite - element techniques are used as one type of mesh approach to solve these PDE (Dehghan 2005, Dehghan 2006a, Dehghan 2006b). The suitability of these techniques is constrained by provisional stabilisation of explicit finite - element processes and the requirement for extensive CPU usage in implicit finite difference arrangements, despite the fact that they are efficient for attempting to solve different types of PDEs. The suitability of these techniques is constrained by provisional stabilisation of clear and specific finite - element processes as well as the requirement for extensive CPU time in finite - difference arrangements, despite the fact that they are efficient for solving different types of PDEs. Additionally, only mesh points derived from such approaches may be used to produce a numerical solution (Dehghan 2006b) and the efficiency of these well-known approaches is decreased in nonsmooth and specially - designed environments. The space-fractional convective migration issue was solved by certain authors using the Legendre-Gauss-Lobatto interpolation technique and the Chebyshev-tau technique, and they obtained extremely precise results (Bhrawy and Baleanu 2013, Ren *et al.* 2013).

In order to prevent mesh formation, meshfree approaches have actually caught the interest of academics. The component free Galerkin technique, the replicating core particles, the point approximation, and other meshless approaches are a few examples. View (Liu and Gu 2004) and its sources to get a more detailed overview. To use the mesh-free approach, Dehghan and Shokri computed the second order telegraph formulas with constants (Dehghan and Shokri 2008).

A well-known and effective approximation technique for the interpolation of dispersed data is the use of radical kernel function (RKFs). The utilization of RKFs to solve approximate methods to partial differential equations is founded on the collocation technique and is a meshfree technique. The main benefit of numerical operations employing RKFs over conventional methods is meshfree. Samples of how RKFs are effectively employed to solve PDEs may be seen in (Kansa 1990, Zerroukat *et al.* 1998, Li *et al*. 2010, Jiang *et al.* 2012, Jiang *et al.* 2013).

Several scientists and engineers have been interested in the RKFs technique's development over the past 10 years as a genuinely meshfree method for estimating partial derivative equation solutions. Multiple scholarly publications have been produced, and also the meshfree approach has grown in importance (Atluri and Shen 2002, Liu, G and Liu, M 2003, Griebel 2005, Liu and Gu 2005, Fasshauer 2007, Ferreira *et al.* 2009, Liu 2009).

In this thesis, we describe a web technique with RKFs for cooperating time-dependent issues controlled by third- and fourth-order telegraph equations. To verify the high accuracy of the proposed method, the outcomes of the numerically trials are provided and contrasted with the exact solution.

2.1 Partial Differential Equations

PDEs which are discovered to properly simulate physical processes like thermal expansion, acoustic waves, and several others, are often the source of issues for such instruments. Despite simple algebraic formulas, DEs link a functional to its derivatives. As instance, $u'(x) = u(x)$.

ODEs and PDEs are two categories of DEs. The derivatives of a single value, in this case x, is a constituent of an ODE. Partial derivatives and numerous parameters, including such $u_{xx}(x,t)$, will be included in a PDEs.

According to the highest included derivative, the symbol u_{xx} is categorised as belonging to a specific category. The two instances above come first and second, correspondingly (Renardy and Rogers 2006).

Just one component in a homogenous differential equation are those that depends on the arbitrary function, as in the preceding instances. Non-homogeneous refers to a formula that has components that don't dependent on the arbitrary function. The formula $u_t(x\,,t) - u_{xx}(x,t) = f\,(\,x,y\,)$ which has an additional term frequently referred to as the pushing component, is an illustration of a non-homogeneous formula. Non - homogeneous physical domains or spatially explicit properties of the material might be a secondary source of complication.

Another crucial element of DEs is constrains, that further restrict solutions. For instance, $u'(x) = u(2x)$ may have a solution of $u(x) = 6e^{2x}$, however a condition like $u(0) = 1$ would limit the possible solutions.

The Dirichlet and Neumann initial conditions would be applied to the large majority of the results in this essay. 1st BCs, also known as Dirichlet initial conditions, limit the functionality of the function at specific points.

It rapidly becomes exceedingly difficult to solve huge physical systems that may be described by PDEs, necessitating a complex approach and expensive machines. The solution domain for these models is split into smaller chunks, or parts, and the collection of these components is known to as a meshes. The "form" functions, which represents the variability of a variables across a component of the meshes, is used in the mesh construction to numerically estimate the proper derivatives for models. As a result, a form matrix Ω and a vector U, comprising the system parameters that must be solved, are produced.

The standard method for a moment result would entail decomposing or inverting the form matrices and performing the proper matrices multiplication operation to find the fields parameters. For instance, the result to the formula $\frac{\partial^2}{\partial x^2} U = \Phi \Longrightarrow \Omega_{xx} \mathrm{U} = \Phi$, would've been $U = \Omega_x x^{-1} \Phi$. When dealing with just a moment result, one should continuously use a fixed or adjustable elapsed time and a moment approach to resolve the systems formula. Time skipping techniques often are divided into two classifications: implicitly, that inverts the matrices, or explicitly, with no invert the matrices and employs straightforward matrix multiplication operation (Vlach *et al.* 1983).

These sorts of time skipping techniques include benefits and drawbacks, and numerous of them will be employed in this study along with thorough arguments. The various techniques all have advantages in terms of performance, efficiency, and memory usage. For instance, due to the electric and magnetism fields directions, a complete matrix Maxwell formula result necessitates a matrix with proportions six times bigger than those of a sub clause. Therefore, in a vector illustration three-dimensional space, matrices invert may become rather expensive. By eliminating the necessity for a matrix multiplication or deconstruction, an exponential time skipping technique is more useful for solving such huge problems.

2.2 Using a Mesh to Solve PDEs

The three basic techniques discussed here are collectively referred to as "meshed techniques" since they all need a mesh produced utilizing rigid geometrical guidelines and previous knowledge of form functions. Every meshed approach even has advantages and disadvantages each of its own. These techniques are the Boundary Element Technique, the Finite Element approach (FEA) and the Finite Difference approach (FDA). Every approach makes an effort to identify the unidentified parameter value in a given area of focus. The complete computational environment that must be partitioned and resolved constitutes the topic.

2.2.1 Method of finite differences

The approach to be explained that is thought to be easiest to use and execute is FDM. This approach involves dividing the supplied systems into a grid pattern and relies just on difference between the grids to arrive at a solution immediately. The mesh encompasses the full mathematical model and takes up the entire grids. To get the estimated gradient, divide the change in the fields at two adjacent vertices by their proximity. This operation can be utilized as a derivatives operation in the form matrix. A prime example of a differences technique employing the central-difference approximations both for first and 2nd order derivatives in (Smith 1974).

$$\begin{aligned} u'(x_0) &\approx \frac{1}{2r}(u(x_0+r)-u(x_0-r)) \\ u''(x_0) &\approx \frac{1}{r^2}(u(x_0+r)-2u(x_0)+u(x_0-r)), \end{aligned} \tag{2.1}$$

where r is the grid size, and x_0 is the position of the derivatives of both for first and 2nd order derivatives $u'(x_0)$ and $u''(x_0)$, respectively in (2.1). Below in Figure 2.1, you can see an illustration of an FD mesh. Although this mesh is uniform and has a fixed grid size, it may be altered to have different densities in different areas. As shown in Figure 2.2, this uneven meshing frequently results in an excess of nodes along the coordinate axes.

In order to simulate curving contours, approximate approaches and extremely high densities are needed, which limits the typical grid to a rectangular design. These can greatly increase both the quantity of nodes and the amount of processing required to solve an issue.

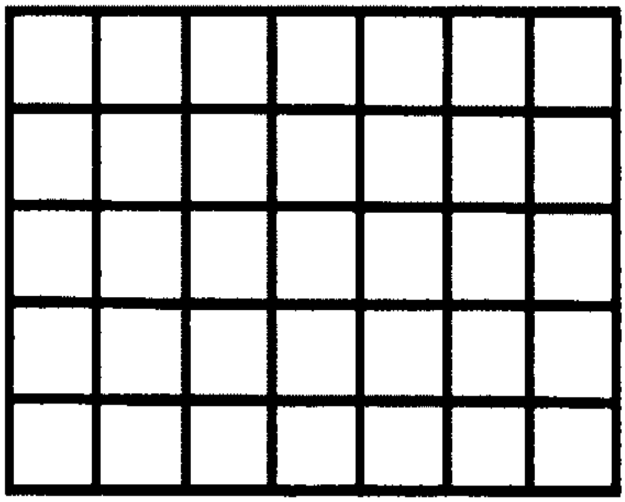

Figure 2.1 A Finite Difference Mesh illustration.

It is feasible to utilize irregular grids, but the concept is not properly suited for such situations and mesh generation might get challenging very soon.

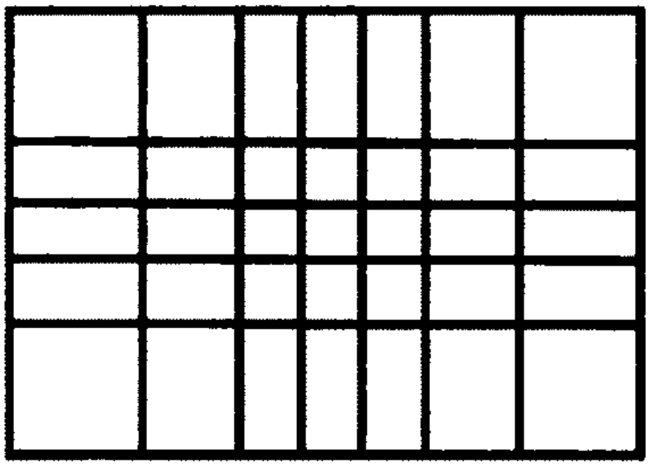

Figure 2.2 An illustration of a finite difference meshes with a somewhat off-center grid. Around the area boundary, there are smaller population spots with greater density spots.

The study of uneven FD grids is still under investigation (Smy *et al.* 2001).

2.2.2 Meshes have issues

Each 3 of these techniques have undergone extensive investigation and have found utility in both professional and educational settings. Every one of these approaches has a major disadvantage due to the labor-intensive process involved in creating the mesh required to create a solution. The pattern in FDA is extremely regular and often utilizes the same grid thickness across the whole area. Also with basic geometries, this results in an extremely high amount of points, which is undesired. The merger of grids may modify density, but developing these methods and working with various assumptions can make the procedure challenging. The shapes are also limited to rectilinear designs, which need assumptions and several extra points for curved designs.

FDA is less able to accommodate curved designs than FEA and also can manage significant variations in component density. The property's geometry must be thoroughly understood, and the area meshing methods must be fairly sophisticated. It can be challenging to write the meshing process that produces and fits the preset form elements, and automatic meshing for complicated geometries is typically not among the finest quality.

Even as components deform and no longer precisely approximate their own forms, PDEs calculating for tension and stress fail. Testing for failure point and fracturing are only permitted at the interfaces of predefined components. It is feasible to iteratively remeshing the subdomains, but the accuracy of the result suffers as a result of the approximations. The mesh generation process requires a lot of processing since it is not possible to just layer on some more triangular because the geometry relationships and components need to be recalculated. Using FEA and mesh-based techniques, adaptive meshing is especially challenging in 3 components. Contrary to FDA or FEA's sparse matrices, BEA systems often produce dense operators' matrix. The decomposition of such matrix is theoretically far more challenging than that of their scanty equivalents.

2.3 Approximation Using RKF

A combination of H radial kernel functions can be used to approximate a distributions $\Phi(x)$ using RKFs, and this formula often looks like this:

$$\Phi(x) \simeq \sum_{n=1}^{H} \zeta_n \phi(x, x_{\,n}) + \omega(x), \quad \text{for } x \in \theta \subset R^{\iota}, \tag{2.2}$$

where H represents the total number of data sets, $x = (x_1, x_2, \dots, x_i), i$ is the situation's size, the undetermined values are denoted by the ζ and ϕ is the radial kernal function. It is possible to write (2.2) without any of the extra polynomial. In this scenario, ϕ must have a positive definite function to ensure that the ensuing situation can be solved. Nevertheless, if ϕ is unconditionally positive definite, that really is ψ, when ϕ has a polynomial development to infinitely, is often necessary. RKFs, which are described as:

Reverse multiquadric (RMQ): $\phi(\boldsymbol{x}, \boldsymbol{x_j}) = \frac{1}{\sqrt{\delta_n^2+\kappa^2}}, \kappa > 0.$

splines on flat sheets (SFS): $\phi(\boldsymbol{x}, \boldsymbol{x_j}) = \delta_n^{2\sigma} \log(\delta_n), \ \sigma = 1,2,3, \dots,$

The radial basis function of the RMQ has the type $1/\sqrt{\delta^2 + \kappa^2}, \kappa > 0$. The selection of constant κ has a significant impact on the correctness of the numerical method so an inappropriate value κ will result in a single interpolation matrices. Additionally, the accuracy might be impacted by the quantity of nodes that are selected. Anyone may learn more about RKF's methodology by reading (Schaback 1995, Wu and Schaback 1993).

The polynomials $\omega(x)$ in (2.2) is often expressed in the way if $\mathfrak{R}_j^i$ represents the space of i- change polynomial of order not exceed j and the polynomials $\wp_1, \wp_2, \dots, \wp_m$ are the foundation of $\mathfrak{R}_j^i$ in R^i as follows:

$$\omega(x) = \sum_{\mathrm{i}=1}^{r} \gamma_i \wp_i(x_j), \tag{2.3}$$

where $r = (j - 1 + i)!/(i!\,(j - 1)!)$.

Using the geolocation approach, the parameters $(\zeta_1, \zeta_2, \dots, \zeta_H)$ and $(\gamma_1, \gamma_2, \dots, \gamma_r)$, are obtained in equation. Nevertheless, additional r formulas are needed in contrast to the H formulas that emerge by collocating at the H locations and putting $\omega(x) = 0$ in Equation (2.3). The r requirements make sure of this.

$$\sum_{j=1}^{H} \gamma_i \wp_i(x_j) = 0,\ i = 1,2, \dots, r. \tag{2.4}$$

Assuming ℓ is just a linear partial differential operation, by taking ℓu to both sides of Equation (2.2) and putting $u(x) = \Phi(x)$ in equation (2.4) we obtain

$$\ell u(x) \simeq \sum_{j=1}^{H} \zeta_j \ell \phi(x, x_j) + \ell \omega(x), \tag{2.5}$$

where $\omega(x)$ is expressed in the way if $\Re_j^i$ represents the space of *i*- change polynomial of order not exceed *j*, ℓ is a linear partial differential operation, ζ_j is the radial kernel function and $\phi(x, x_j)$is splines on flat sheets in (2.5).

3. HIGHER ORDER PARTIAL DIFFERENTIAL EQUATIONS

3.1 Weak Formulations

A BVP (3.1) has solution $\lambda \in C^2(\phi)$ often requires adequate regular of the issue and could not exist in the traditional way. Alternatively, by multiplying each parts by the a test $\theta \in H_0^2(\phi;\mathbb{R})$ and integrated by part, we take into account the weak construction of (3.1):

$$\begin{cases} (\mathrm{M}[u],\theta) \triangleq \int_\Omega \left(\sum_{j=1}^{k} \sum_{i=1}^{k} m_{ij}\,\partial_j u\,\partial_i \phi + \sum_{i=1}^{k} n_i \theta\,\partial_i u + \lambda \mathrm{u}\,\theta - \xi\theta \right) \mathrm{d}x = 0, \\ \mathrm{N}[u] = 0, \text{ on } \partial\phi \end{cases} \tag{3.1}$$

where $m, n \in \Re^{k,k}$ with $H_0^2(\phi; \mathrm{R})$ stands for the Sobolev spaces, which is a Hilbert space of function whose weak partial derivatives and they are L^2 capable of approximating on ϕ without vanishing traces on the $\partial\phi$. Keep in mind that because $\theta = 0$ on $\partial\phi$ the boundaries parts of (3.1) vanish after section integrating. If for any $u \in H^2(\phi;\mathbb{R})$ with potentially positive real traces fulfils (3.1) for every $\varphi \in H_0^2$, we argue as u is a poor solution of (3.1). A poor solution to a problem is typically possible but a formal approach is not always. Thus, in this study, we look for the weak solution denoted by (3.1) in order to answer a BVP (3.1) as well as can, despite the fact that it doesn't accept a resolution in the classic way.

3.2 Minimizing Induced Operator Norms

It is possible to consider the following as an unique viewpoint for the weak solution u. As a linear functional (operation), we may think of $M[u]: H_D^2(\phi) \to \mathbb{R}$ so that $M[u](\theta) \triangleq \langle M[u] - 1, \theta - 1 \rangle$, as given in (3.1). Afterward, the formulation of the operators norms of $M[u]$ generated by the L^2 norm is

$$\| M[u] \|_s \triangleq \mathrm{m} \ \{\langle M[u] - 1, \theta - 1\rangle / \| \theta \|_2 | \ \theta \in H_0^2, \theta \neq 0\} \tag{3.2}$$

and $\| \theta - 1 \|_2 = \left(\int_\phi |\theta(x) - 1|^2 \, \mathrm{d}x\right)^{1/2}$. As a result, u only provides a weak solution to (3.1) if and only if $\| M[u] \|_s = 0$ and the border constraint $N[u] = 0$ is met on $\partial\phi$. A weak solution u to (3.1). Therefore resolves the two additional identical issues in observation of (3.2), and this is known simply $\| M[u] \|_s \geq 0$. The next argument provides an overview of this conclusion.

Remark 3.2.1. If u^* meets the boundary requirement $N[u^*] = 0$, then u^* is a weak result of the Equation (3.1) if and only if u^* resolves the issues in (3.2) and $M[u^* \ | \|_s = 0$.

Before anything more, we'll solve several examples of non-homogeneous time-dependent problems.

3.3. Issues with Non - homogenous Time Derivative

Assume the time-dependent of order five issue below is an example:

$$\begin{aligned} u_{ttttt} + \lambda\beta u_{tttt} + \zeta\beta u_{ttt} + \mu\beta u_{tt} + \nu\beta u_t & \\ = o g_1(x) u_{xxxxxx} + \eta g_2(x) u_{xxxxx} + \upsilon g_3(x) u_{xxx} + \sigma g_4(x) u_{xx} & \\ + \kappa\beta u_x + g_5(x,t), & \end{aligned} \tag{3.3}$$

where $\lambda, \zeta, \mu, \nu, o, \eta, \upsilon, \sigma, \kappa$ are constants and $x \in \phi \cup \partial\phi = [\lambda_1, \xi_1] \subset R, \ 0 < t < T$, that appears in (3.3).

The initial circumstances as follows:

$u(x, 0) = z_1(x), x \in \theta$

$u_t(x, 0) = z_2(x), x \in \theta$

$$u_{tt}(x,0) = z_3(x), x \in \theta$$

$$u_{ttt}(x,0) = z_4(x), x \in \theta \qquad (3.4)$$

$$u_{tttt}(x,0) = z_5(x), x \in \theta,$$

where $z_1(x), z_2(x), z_3(x), z_4(x)$ and $z_5(x)$ are parameters in (3.4). Furthermore, it fulfills the Dirichlet condition

$$u(x,t) = z(x,t),\ x \in \partial\theta, 0 < t \leq T, \qquad (3.5)$$

where $\lambda, \xi,$ and κ are constant coefficients, and the functions $g_1(x), g_2(x,t), g_3(x), g_4(x), g_5(x), z_1(x), z_2(x), z_3(x), z_4(x), z_5(x),$ and $z(x,t)$ are established, but $u(x,t)$ is the undetermined function. The discretization of Formula (3.3) utilizes the -weighted strategy and using (3.5) as follows:

$$\begin{aligned}
&\frac{u(x,t+dt) - 2u(x,t) + u(x,t-dt)}{(dt)^5} \\
&\quad + \lambda\beta \frac{u(x,t+dt) - 2u(x,t) + u(x,t-dt)}{(dt)^4} \\
&\quad + \zeta\beta \frac{u(x,t+dt) - 2u(x,t) + u(x,t-dt)}{(dt)^3} \\
&\quad + \mu\beta \frac{u(x,t+dt) - 2u(x,t) + u(x,t-dt)}{(dt)^2} \\
&\quad + \nu\beta \frac{u(x,t+dt) - u(x,t-dt)}{2dt} \\
&\quad = \theta[bg_1(x)\Delta u(x,t+dt) + c\alpha u(x,t+dt)] + (1 \\
&\quad - \theta)[bg_1(x)\Delta u(x,t) + c\alpha u(x,t)] + g_2(x,t+dt),
\end{aligned} \qquad (3.6)$$

when the time interval length is $0 \leq \theta \leq 1$, the Laplace operation is Δ, but by using formula $t^{n+1} = t^n + dt$ and $u^{n+1} = u(x, t^{n+1})$ in Equation (3.6) we can obtain:

$$\left(1+\lambda\beta(dt)^4+\zeta\beta(dt)^3+\mu\beta(dt)^2+\nu\beta\frac{dt}{2}\right)u^{n+1}$$
$$\begin{aligned}&-\left(og_1(x)+\eta g_2(x)+\upsilon g_3(x)+\sigma g_4(x)+\kappa\beta u\right)\Delta u^{n+1}\\&=(2+c\alpha(1-\theta)dt^2)\Delta u^n\\&=\left(1+\beta(\lambda(dt)^4+\zeta(dt)^3+\mu(dt)^2+\nu\frac{dt}{2})\right)u^{n+1}\\&-\left(og_1(x)+\eta g_2(x)+\upsilon g_3(x)+\sigma g_4(x)+\kappa\beta u\right)\Delta u^{n+1},\end{aligned}\tag{3.7}$$

where λ, ζ, μ, o, η, υ , κ and c are constant coefficients, and the other functions defined above.

Assume that there exists $L-1$ approximation spots altogether then, $u^{n+1}(x)$ in (3.7) may be roughly represented as

$$u^{n+1}(x)=\sum_{j=1}^{L-1}\zeta_j^{n+1}\phi(\delta_{ij})+\zeta_L^{n+1}x+\zeta_{\mathrm{L}+1}^{n+1},\tag{3.8}$$

where ζ_j^{n+1} is the radial kernel function in (3.8) at each spot $x_i, i=1,2,\dots,L-2$, the interpolation technique is employed to calculate the parameters $(\zeta_1,\zeta_2,\dots,\zeta_{N-1},\zeta_L)$. Therefore, we achieve

$$u^{n+1}(x_i)=\sum_{j=1}^{\mathrm{L}-2}\zeta_j^{n+1}\phi(\delta_{ij})+\zeta_L^{n+1}x_i+\zeta_{\mathrm{L}+1}^{n+1},\tag{3.9}$$

where $\delta_{ij}=\sqrt{\left(x_i-x_j\right)^2}$ and $\zeta_L^{n+1},\zeta_{\mathrm{L}+1}^{n+1}$ are parameters in (3.9). The increased requirements resulting from (2.4) may be expressed as

$$\sum_{j=1}^{\mathrm{L}-2}\zeta_j^{n+1}=\sum_{j=1}^{\mathrm{L}-2}\zeta_j^{n+1}x_j=0,\tag{3.10}$$

where ζ_j^{n+1} is the radial kernel function and putting (3.10) into a matrix, we can write

$$[u]^{n+1} = \mathrm{K}[\zeta]^{n+1}\,, \tag{3.11}$$

where $K = \left[k_{ij}, 1 \leq i, j \leq L\right]$ and

$$[u]^{n+1} = [u_1^{n+1}, u_2^{n+1}, \ldots, u_{L-2}^{n+1}, 0,0,0]^T, [\zeta]^{n+1} = [\zeta_1^n, \zeta_2^{n+1}, \ldots, \zeta_L^{n+1}]^T,$$

where $K = \left[k_{ij}, 1 \leq i, j \leq L\right]$ in (3.11) is denoted by the following form:

$$\mathrm{K} = \begin{pmatrix} \phi_{11} & \cdots & \phi_{1(\mathrm{L}-1)} & x_1 & 1 \\ \vdots & \ddots & \vdots & \vdots & \vdots \\ \phi_{(\mathrm{L}-1)1} & \cdots & \phi_{(\mathrm{L}-1)(\mathrm{L}-1)} & x_{L-1} & 1 \\ x_1 & \cdots & x_{L-1} & 0 & 0 \\ 1 & \cdots & 1 & 0 & 0 \end{pmatrix}.$$

The $L \times L$ matrices K may be divided into $K = K_\mu + K_\nu + K_\xi$ if it contains $m < L - 2$ inner spots and $L - 2 - m$ border points, where $K_\mu, K_\nu and\ K_\xi$ are defined as follows:

$$k_\mu = \begin{Bmatrix} k_{ij} \text{ for } (1 \leq i \leq m, 1 \leq j \leq L + 1), \\ 0 \text{ elsewhere} \end{Bmatrix}$$
$$k_\nu = \begin{Bmatrix} k_{ij} \text{ for } (m + 1 \leq i \leq L - 1, 1 \leq j \leq L + 1), \\ 0 \text{ elsewhere} \end{Bmatrix}$$
$$k_\xi = \begin{Bmatrix} k_{ij} \text{ for } (L \leq i \leq L + 1, 1 \leq j \leq L + 1), \\ 0 \text{ elsewhere} \end{Bmatrix}. \tag{3.12}$$

When the constraints (3.5) and (3.11) are represented in matrix notation by using symbol $\mathcal{L}\{\mathrm{K}\}$ to denote the matrices that has the same dimensions as K and contains the components $\hat{k}_{ij}$, where $\hat{k}_{ij} = \mathcal{L}\{k_{ij}\}, 1 \leq i, j \leq L + 1$ and by using Equation (3.12) we get

$$\omega[\zeta]^{n+2} = \psi[\zeta]^{n} + \left(1 + \beta(\lambda(dt)^{4} + \zeta(dt)^{3} + \mu(dt)^{2} + \nu\frac{dt}{2})\right)\left[u_{\mu}\right]^{n}$$
$$+dt^{2}[g_{2}]^{n+2} + [\mathrm{W}]^{n+2}, \tag{3.13}$$

where

$$\psi = \left(1 + \beta(\lambda(dt)^{4} + \zeta(dt)^{3} + \mu(dt)^{2} + \nu\frac{dt}{2})\right)\mathrm{K}_{\mu}$$
$$+ \left(og_{1}(x) + \eta g_{2}(x) + \upsilon g_{3}(x) + \sigma g_{4}(x) + \kappa\beta u\right)\left([g_{1}] * \Delta\mathrm{K}_{\mu}\right),$$

$$\omega = \left(1 + \beta(\lambda(dt)^{4} + \zeta(dt)^{3} + \mu(dt)^{2} + \nu\frac{dt}{2})\right)\mathrm{K}_{\mu}$$
$$- \left(og_{1}(x) + \eta g_{2}(x) + \upsilon g_{3}(x) + \sigma g_{4}(x) + \kappa\beta u\right)dt^{2}\left([g_{1}] * \Delta\mathrm{K}_{\mu}\right) + \mathrm{K}_{\nu}$$
$$+ \mathrm{K}_{\xi}, [u_{d}]^{n-1} = [u_{1}^{n}, u_{2}^{n}, \dots, u_{m}^{n}, 0, \dots, 0]^{T},$$

$$[W]^{n+2} = [0, \dots, 0, h_{m+2}^{n+2}, h_{m+3}^{n+3}, \dots, h_{L-1}^{n+1}, 0,0,0]^{T},$$

$$[g_{2}]^{n+1} = [g_{2}^{n+2}(x_{1}), g_{2}^{n+2}(x_{2}), \dots, g_{2}^{n+2}(x_{m}), 0, \dots, 0]^{T},$$

$$[g_{1}] = [g_{1}(x_{1}), g_{1}(x_{2}), \dots, g_{1}(x_{m}), 0, \dots, 0]^{T}.$$

The symbol "*" denotes a multiplication of all the elements in the *i*-th row of matrices $\Delta\mathrm{K}_{\mu}$ by the *i*-th constituent of vector $[g_{1}]$. Applying (3.7) used to the domains elements performed to the boundary points results in Equation (3.13). Thus, (3.13) seems to have the following syntax when $n = 0$:

$$\omega[\zeta]^{2} = \psi[\zeta]^{1} + \left(1 + \beta(\lambda(dt)^{4} + \zeta(dt)^{3} + \mu(dt)^{2} + \nu\frac{dt}{2})\right)\left[u_{\mu}\right]^{-1}$$
$$+ dt^{2}[g_{2}]^{2} + [W]^{2}. \tag{3.14}$$

The second starting constraint can always be employed to approximation u^{-1}. The next initial state of Equation (3.14) are partitioned as follows with this objective:

$$\frac{u^1(x) - u^{-1}(x)}{2dt} = g_2(x),$$

$$\frac{u^1(x) - u^{-1}(x)}{(dt)^2} = g_3(x),$$

$$\frac{u^1(x) - u^{-1}(x)}{(dt)^3} = g_4(x),$$

$$\frac{u^1(x) - u^{-1}(x)}{(dt)^4} = g_5(x)\,, x \in \phi, \tag{3.15}$$

where $g_2(x), g_3(x), g_4(x)$ and $g_5(x)$ are approximate solutions.

By combining (3.14) and (3.15), we obtain the following formula:

$$\omega[\zeta]^2 = \psi[\zeta]^1 + \left(1 + \beta(\lambda(dt)^4 + \zeta(dt)^3 + \mu(dt)^2 + \nu\frac{dt}{2})\right)[\chi]dt^2[g_2]^2 + [W]^2,$$

where $[\chi] = \begin{bmatrix} (g_1)_1, (g_2)_1, (g_3)_1, (g_4)_1, (g_5)_1, \dots, \\ (g_1)_\mu, (g_2)_\mu, (g_3)_\mu, (g_4)_\mu, (g_5)_\mu, 0, \dots, 0 \end{bmatrix}^T$. We can obtain all of the ζ by combining the conditions (3.4) and (3.15); consequently, we may obtain the approximate methods.

We apply the LU decomposition to the coefficients just once and employ this decomposition in our approach because the coefficient matrix is identical in every temporal stage.

4. RESULTS AND DISCUSSION

For purpose of evaluating the effectiveness of the novel approach to solving time-dependent issues defined by the PDEs, several numerical solutions are presented in this chapter.

Application 4.1 Consider the following PDEs:

$$u_{tttt} + u_{ttt} + u_t = e^{2x} u_{xxx} + 7u_x + g_2(x,t),\ 0 < x < 1, t > 0, \tag{4.1}$$

where u_{tttt}, u_{ttt}, u_t are the fourth , third and first derivative of u. By comparing (4.1) with (3.3) then, $u_{tt} = 0 = u_{xxxx} = u_{xx}, \lambda = \zeta = \nu = 1, \mu = 0 = o = \sigma = \eta, \upsilon = 1, \kappa = 7$ and $g_1(x) = e^{2x}$; $g_2(x,t) = [x(1 - x + x^2)(1 - t + t^2 + t^3) + e^{2x} t^4] e^{-2t}$, with initial conditions

$$\begin{aligned} &u(0,t) = 0,\ t > 0, \\ &u(1,t) = 0,\ t > 0, \\ &u(2,t) = 0,\ t > 0, \\ &u(3,t) = 0,\ t > 0, \\ &u(4,t) = 0,\ t > 0. \end{aligned} \tag{4.2}$$

and

$$\begin{aligned} &u(x,0) = 0,\ 0 \le x \le 1, \\ &u_t(x,0) = 0,\ 0 \le x \le 1, \\ &u_{ttt}(x,0) = 0,\ 0 \le x \le 1, \\ &u_{tttt}(x,0) = 0,\ 0 \le x \le 1, \end{aligned}$$

where $t \in Z^+$. The formula analytical result of Equations (4.1), (4.2) is

$$u(x,t) = x(1 - x + x^2)t^4 e^{-2t}. \quad (4.3)$$

The RMQ and SFS are employed to resolve this issue. For parameters $dx = 0.001$ and $dt = 0.0001$, following findings are obtained. For $t = 1,2,3,4,,5,6$ and 7, Table 4.1 lists the L_∞ , L_2, and RMS of Equation (4.3).

Table 4.1 Numerical errors using RMQ ($\lambda = 0.08$) and SFS ($m = 6$) represented at different times, where $dx = 0.001$ and $dt = 0.0001$.

T	L_∞		L_2	
	RMQ	**SFS**	**RMQ**	**SFS**
1	7.2874×10^{-6}	7.6395×10^{-6}	4.0292×10^{-5}	3.391×10^{-5}
2	4.1076×10^{-4}	5.7215×10^{-4}	2.7391×10^{-6}	5.1672×10^{-6}
3	5.8234×10^{-4}	4.7247×10^{-4}	7.4207×10^{-4}	4.8251×10^{-4}
4	3.7206×10^{-5}	5.827×10^{-5}	6.8207×10^{-5}	5.827×10^{-5}
5	1.835×10^{-6}	3.9204×10^{-6}	3.8261×10^{-6}	6.8017×10^{-6}
6	7.0264×10^{-5}	5.371×10^{-5}	1.9477×10^{-5}	4.0383×10^{-5}
7	3.1071×10^{-6}	5.2615×10^{-6}	6.3511×10^{-4}	7.2528×10^{-4}

We also provide an RMQ assessment of a parameter estimate λ for outcomes. The L_∞ and L_2 errors using various λ at period $t = 5$ are displayed in Table 4.2.

Table 4.2 Numerical mistakes employing RMQ at time $t = 5$ where $dx = 0.001, dt = 0.0001$ are expressed by a separate value λ

λ	L_∞	L_2	**RMQ**
0.0	6.7528×10^{-4}	5.2913×10^{-4}	7.1942×10^{-4}
0.02	4.7626×10^{-6}	6.2604×10^{-5}	4.8291×10^{-5}
0.04	8.6322×10^{-5}	3.2081×10^{-4}	6.2041×10^{-4}
0.06	3.7297×10^{-3}	7.2951×10^{-4}	5.2702×10^{-4}
0.08	7.5280×10^{-6}	6.2861×10^{-6}	7.9263×10^{-6}

The space-time graphs of the numerical findings using RMQ ($\lambda = 0.08$) for $t = 1,2,3,4,,6$ and 7 with $dx = 0.001$ and $dt = 0.0001$. The findings collected demonstrate the current approximation scheme's excellent precision and efficiency. It should be noted that in Figure 4.1, we are unable to tell the exact solution in addition to the approximated result.

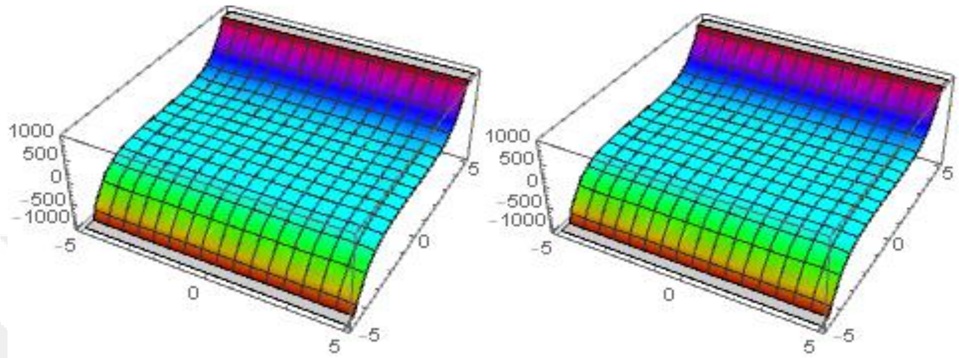

(a) exact solution at t=1 *(b) approximat solution at t=1*

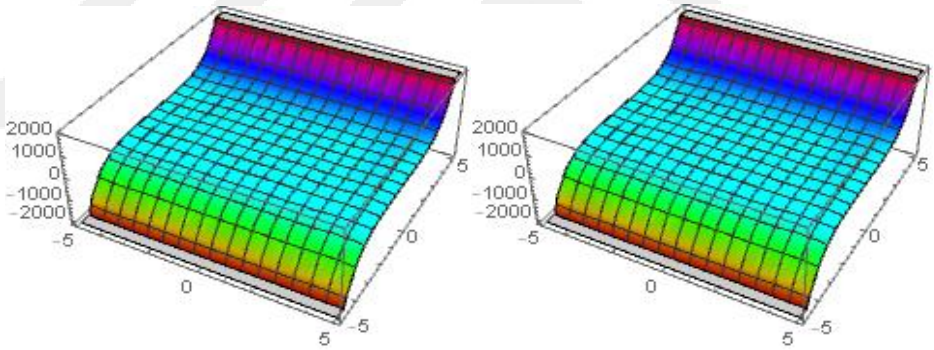

(c) exact solution at t=2 *(d) approximat solution at t=2*

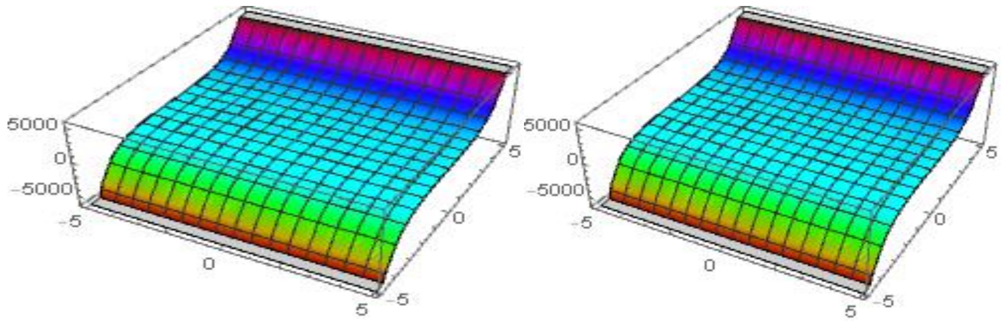

(e) exact solution at t=3 *(f) approximat solution at t=3*

Figure 4.1 RMQ ($\lambda = 0.08$) is used in the area graphs of the numerical solutions at time $t = 1,2,3,4,5,6$ and 7 with $dx = 0,001$ and $dt = 0.0001$.

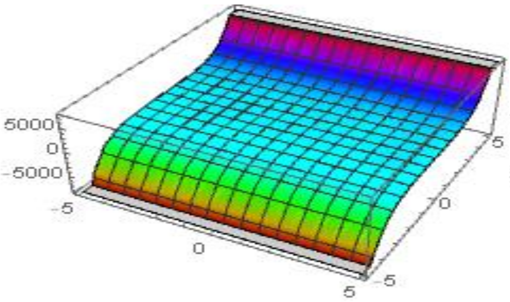

(g) exact solution at t=4

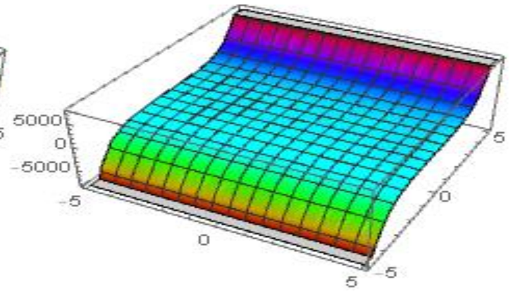

(h) approximat solution at t=4

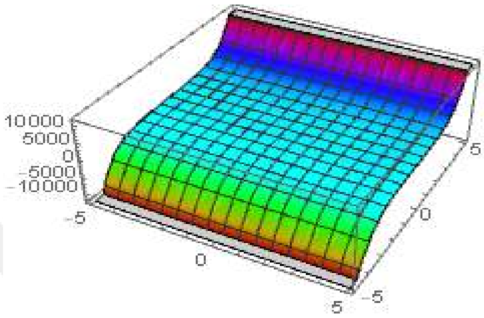

(i) exact solution at t=5

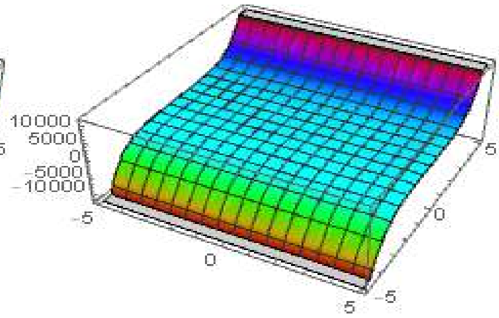

(j) approximat solution at t=5

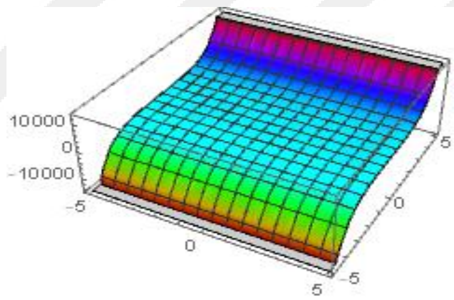

(k) exact solution at t=6

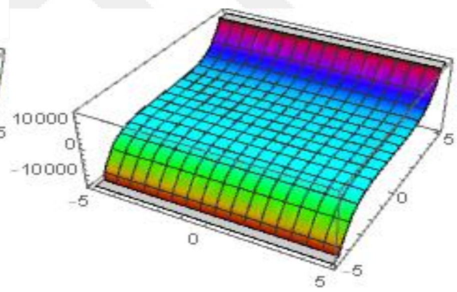

(l) approximat solution at t=6

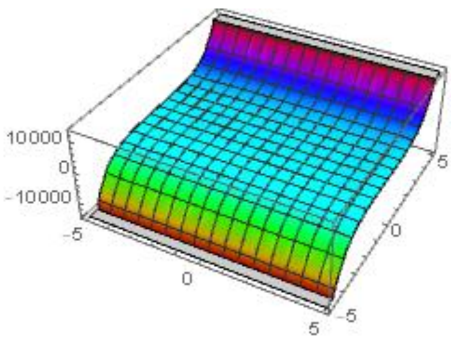

(m) exact solution at t=7

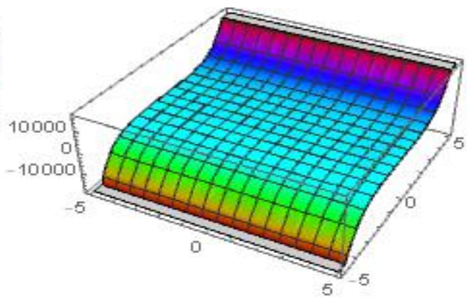

(n) approximat solution at t=7

Figure 4.1 (Continued) RMQ ($\lambda = 0.08$) is used in the area graphs of the numerical solutions at time $t = 1,2,3,4,5,6$ and 7 with $dx = 0,001$ and $dt = 0.0001$.

Application 4.2 Consider the following PDEs:

$$u_{tttt} + u_{ttt} + u_t = (x^2 + 1)u_{xxx} - 3u_x + g_2(x,t),\ 0 < x < 1, t > 0. \tag{4.4}$$

By comparing (4.4) with (3.3) then, $u_{tt} = 0 = u_{xxxx} = u_{xx}, \lambda = \zeta = \nu = 1, \mu = 0 = o = \sigma = \eta, \upsilon = 1, \kappa = 3$ and $g_1(x) = e^{2x}$; $g_2(x,t) = [(1 - x + x^2)(1 - t + t^2 + t^3) + (1 + x^2)t^4]e^{-2t}$

with initial conditions

$$\begin{aligned} &u(0,t) = 0,\ t > 0, \\ &u(1,t) = 0,\ t > 0, \\ &u(2,t) = 0,\ t > 0, \\ &u(3,t) = 0,\ t > 0, \\ &u(4,t) = 0,\ t > 0. \end{aligned} \tag{4.5}$$

and

$$\begin{aligned} &u(x,0) = 0,\ 0 \le x \le 1, \\ &u_t(x,0) = 0,\ 0 \le x \le 1, \\ &u_{ttt}(x,0) = 0,\ 0 \le x \le 1, \\ &u_{tttt}(x,0) = 0,\ 0 \le x \le 1, \end{aligned}$$

where $t \in Z^+$. The formula's analytical result of Equations (4.4), (4.5) is

$$u(x,\mathrm{t}) = (1 - x + x^2)t^4 e^{-2t}. \tag{4.6}$$

The RMQ and SFS are employed to resolve this issue. For parameters $dx = 0.001$ and $dt = 0.0001$, following findings are obtained. For $t = 1,2,3,4,,5,6$ and 7, Table 4.3 lists the L_∞ , L_2, and RMS of Equation (4.6).

Table 4.3 Numerical errors using RMQ ($\lambda = 0.09$) and SFS ($m = 7$) represented at different times, where $dx = 0.001$ and $dt = 0.0001$.

T	L_∞		L_2	
	RMQ	**SFS**	**RMQ**	**SFS**
1	5.9264×10^{-5}	6.6251×10^{-5}	5.285×10^{-4}	6.3922×10^{-4}
2	4.927×10^{-6}	2.7207×10^{-5}	6.2064×10^{-5}	3.2752×10^{-5}
3	4.2012×10^{-7}	5.1952×10^{-6}	4.2741×10^{-6}	1.2698×10^{-6}
4	1.3356×10^{-4}	1.7291×10^{-4}	2.9276×10^{-4}	5.2708×10^{-4}
5	4.0165×10^{-6}	6.8304×10^{-6}	3.2765×10^{-5}	4.0829×10^{-5}
6	5.3472×10^{-4}	4.2711×10^{-5}	5.8606×10^{-5}	2.8293×10^{-5}
7	6.8205×10^{-5}	3.7278×10^{-5}	1.9927×10^{-5}	3.8674×10^{-5}

We also provide an RMQ assessment of a parameter estimate λ for outcomes. The L_∞ and L_2 errors using various λ at period $t = 6$ are displayed in Table 4.4.

Table 4.4 Numerical mistakes employing RMQ at time $t = 6$ where $dx = 0.001$ and $dt = 0.0001$ are expressed by a separate value λ

$\boldsymbol{\lambda}$	L_∞	L_2	**RMQ**
0.0	3.6209×10^{-6}	5.2863×10^{-6}	4.8763×10^{-6}
0.02	5.9365×10^{-5}	6.2903×10^{-5}	3.9277×10^{-4}
0.04	6.8624×10^{-4}	2.8255×10^{-4}	2.2032×10^{-4}
0.06	4.8207×10^{-6}	6.3920×10^{-5}	5.7223×10^{-5}
0.08	2.2725×10^{-5}	3.5042×10^{-4}	4.6255×10^{-4}

The space-time graphs of the numerical findings using RMQ ($\lambda = 0.09$) for $t = 2,3,4,,6$ and 7 with $dx = 0.001$ and $dt = 0.0001$. The findings collected demonstrate the current approximation scheme's excellent precision and efficiency. It should be noted that in Figure 4.2, we are unable to tell the exact solution in addition to the approximated result.

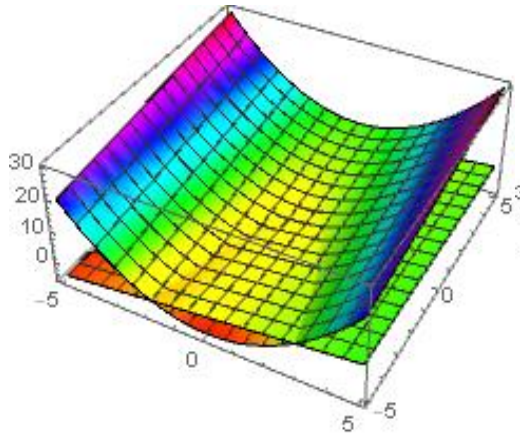

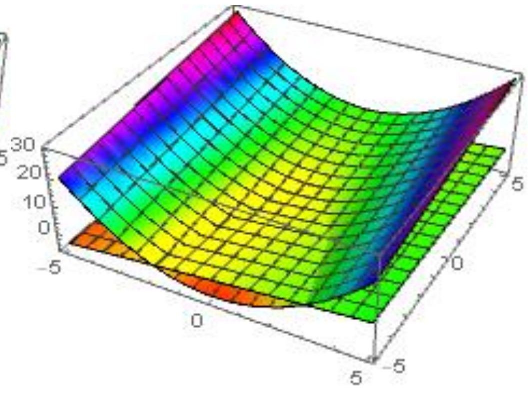

(a) exact solution at t=1 *(b) approximat solution at t=1*

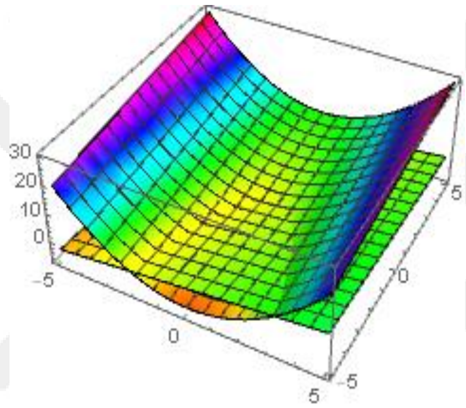

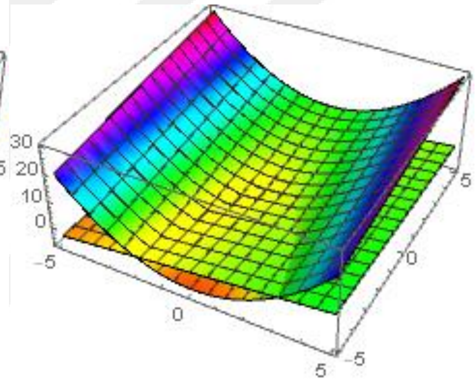

(c) exact solution at t=2 *(d) approximat solution at t=2*

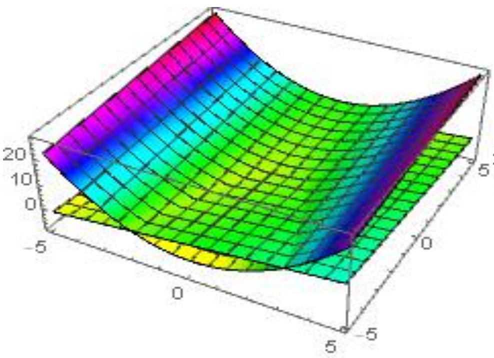

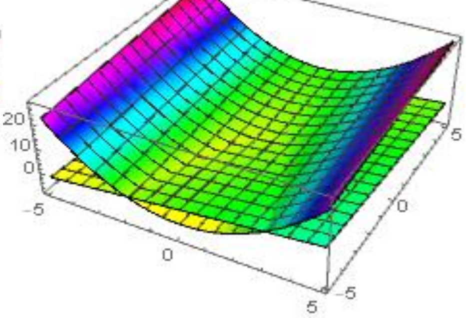

(e) exact solution at t=3 *(f) approximat solution at t=3*

Figure 4.2 RMQ ($\lambda = 0.09$) is used in the area graphs of the numerical solutions at time $t = 2,3,4,5,6$ and 7 with $dx = 0.001$ and $dt = 0.0001$.

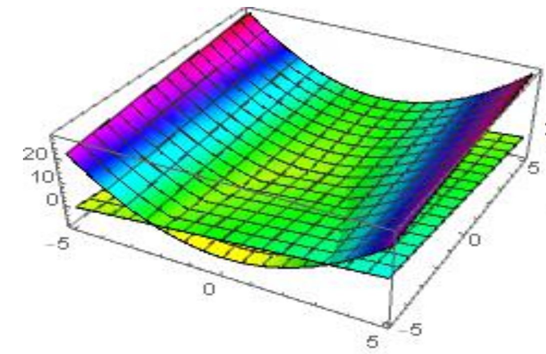

(g) exact solution at t=4

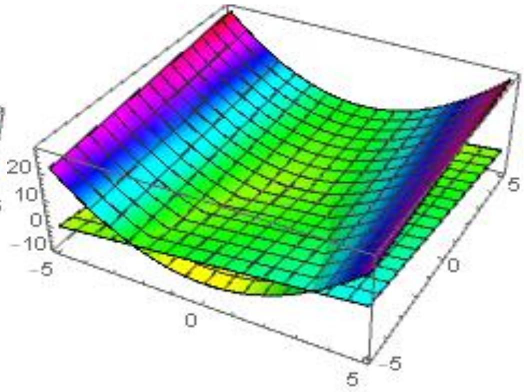

(h) approximat solution at t=4

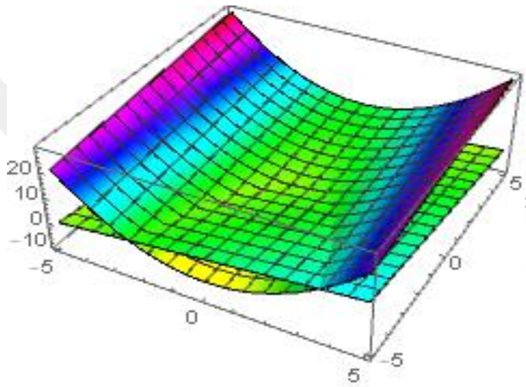

(i) exact solution at t=5

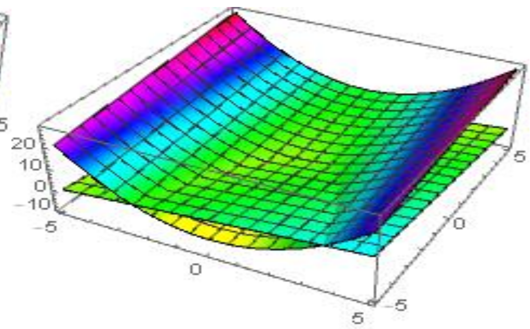

(j) approximat solution at t=5

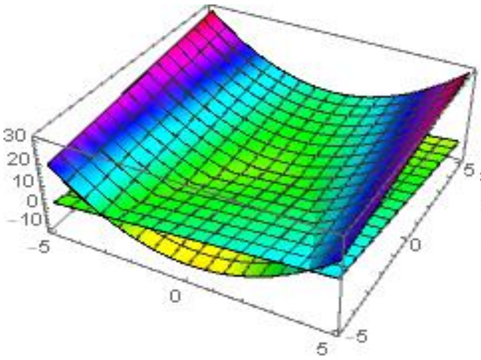

(k) exact solution at t=6

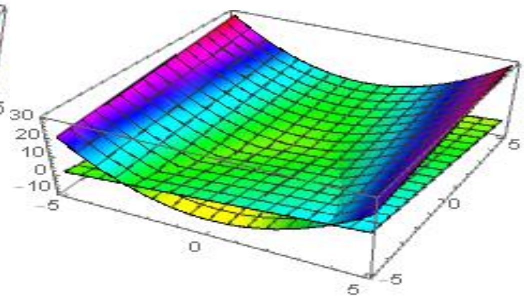

(l) approximat solution at t=6

Figure 4.2 (Continued) RMQ ($\lambda = 0.09$) is used in the area graphs of the numerical solutions at time $t = 2,3,4,5,6$ and 7 with $dx = 0.001$ and $dt = 0.0001$.

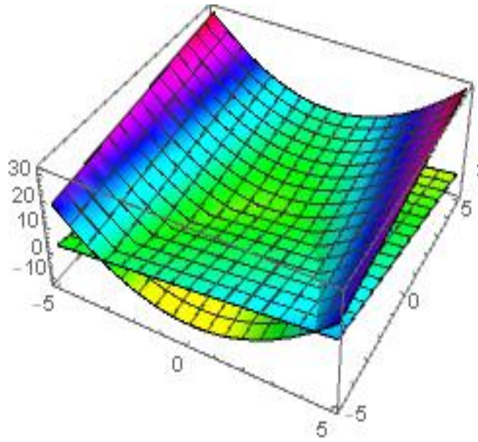

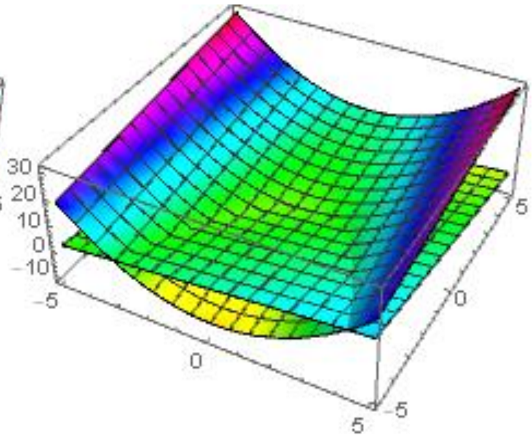

(m) exact solution at t=7 (n) approximat solution at t=7

Figure 4.2 (Continued) RMQ ($\lambda = 0.09$) is used in the area graphs of the numerical solutions at time $t = 2,3,4,5,6$ and 7 with $dx = 0.001$ and $dt = 0.0001$.

Application 4.3 Consider the following PDEs:

$$u_{tttt} + u_{tt} + u_t = u_{xxx} + u_{xx} + 7u_x + g_2(x,t),\ 0 < x < 1, t > 0. \tag{4.7}$$

By comparing (4.7) with (3.3) then $u_{ttt} = 0 = u_{xxxx}, \lambda = \mu = \nu = 1, \zeta = 0 = o = \eta, \sigma = \upsilon = 1, \kappa = 7$, and; $g_2(x,t) = (1 + \pi^4)e^{-t}\cos(\pi x)$ with initial conditions

$$u(0,t) = 0,\ t > 0,$$
$$u(1,t) = 0,\ t > 0,$$
$$u(2,t) = 0,\ t > 0,$$
$$u(3,t) = 0,\ t > 0,$$
$$u(4,t) = 0,\ t > 0$$

and

$$u(x,0) = \cos(\pi x),\ 0 \le x \le 1,$$
$$u_t(x,0) = -\frac{1}{2}\cos(\pi x),\ 0 \le x \le 1,$$
$$u_{tt}(x,0) = -\frac{1}{2}\cos(\pi x),\ 0 \le x \le 1 \tag{4.8}$$

$$u_{tttt}(x,0) = -\frac{1}{2}\cos(\pi x),\ 0 \le x \le 1.$$

The formula's analytical result of both Equations (4.7), (4.8) is

$$u(x,\mathrm{t}) = e^{-2t}\cos(\pi x). \tag{4.9}$$

The RMQ and SFS are employed to resolve this issue. For parameters $dx = 0.001$ and $dt = 0.0001$, following findings are obtained. For $t = 1,2,3,4,,5,6$ and 7, Table 4.5 lists the L_∞ , L_2, and RMS and Equation (4.9).

Table 4.5 Numerical errors using RMQ ($\lambda = 0.09$) and SFS ($m = 6$)) represented at different times, where $dx = 0.001$ and $dt = 0.0001$.

T	L_∞		L_2	
	RMQ	**SFS**	**RMQ**	**SFS**
1	3.7427×10^{-6}	5.0261×10^{-6}	2.8499×10^{-5}	5.7256×10^{-5}
2	7.1842×10^{-6}	6.8382×10^{-6}	3.9522×10^{-6}	4.2763×10^{-6}
3	5.8110×10^{-4}	3.7266×10^{-4}	7.2844×10^{-5}	2.9903×10^{-5}
4	2.6255×10^{-5}	4.0623×10^{-5}	1.8772×10^{-4}	6.2207×10^{-4}
5	1.7482×10^{-6}	2.8207×10^{-6}	5.4083×10^{-6}	1.6331×10^{-6}
6	4.1915×10^{-6}	3.9207×10^{-6}	4.7290×10^{-6}	3.6526×10^{-6}
7	5.7260×10^{-5}	6.7622×10^{-5}	3.5928×10^{-5}	6.7319×10^{-5}

We also provide an RMQ assessment of a parameter estimate λ for outcomes. The L_∞ and L_2 errors using various λ at period $t = 6$ are displayed in Table 4.6.

Table 4.6 Numerical mistakes employing RMQ at time $t = 6$ where $dx = 0.001$, $dt = 0.0001$ are expressed by a separate value λ.

λ	L_∞	L_2	RMQ
0.0	4.8623×10^{-5}	6.0176×10^{-5}	5.2976×10^{-5}
0.02	7.2956×10^{-4}	4.9287×10^{-4}	6.2801×10^{-5}
0.04	6.2865×10^{-6}	3.8640×10^{-6}	2.7629×10^{-6}
0.06	5.2092×10^{-4}	7.0287×10^{-4}	4.2181×10^{-5}
0.08	2.8962×10^{-5}	5.2733×10^{-5}	3.9276×10^{-5}

The space-time graphs of the numerical findings using RMQ ($\lambda = 0.09$) for $t = 2,3,4,6$ and 7 with $dx = 0.001$ and $dt = 0.0001$. The findings collected demonstrate the current approximation scheme's excellent precision and efficiency. It should be noted that in Figure 4.3, we are unable to tell the exact solution in addition to the approximated result.

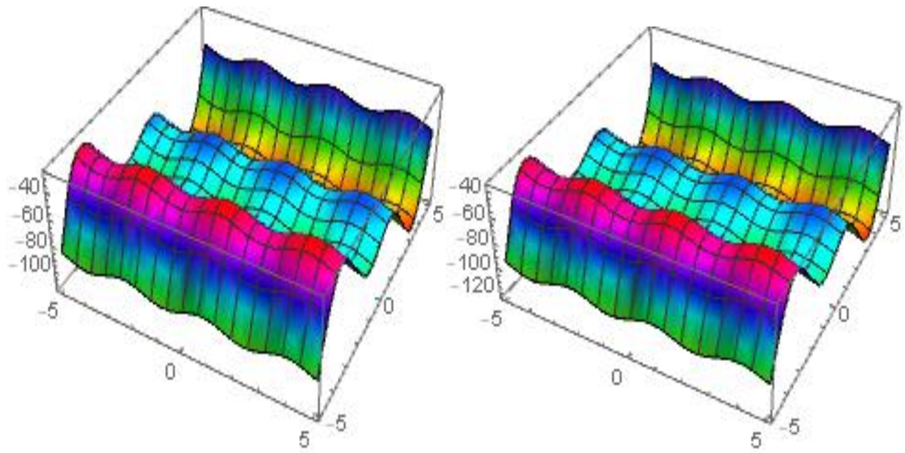

(a) exact solution at t=2 *(b) approximat solution at t=2*

Figure 4.3 RMQ ($\lambda = 0.09$) is used in the area graphs of the numerical solutions at time $t = 2,3,4,5,6$ and 7 with $dx = 0.001$ and $dt = 0.0001$.

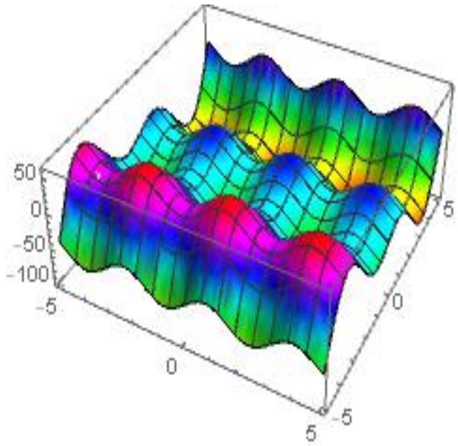

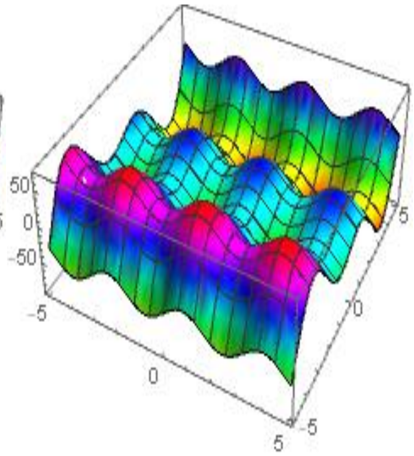

(c) exact solution at t=3 *(d) approximat solution at t=3*

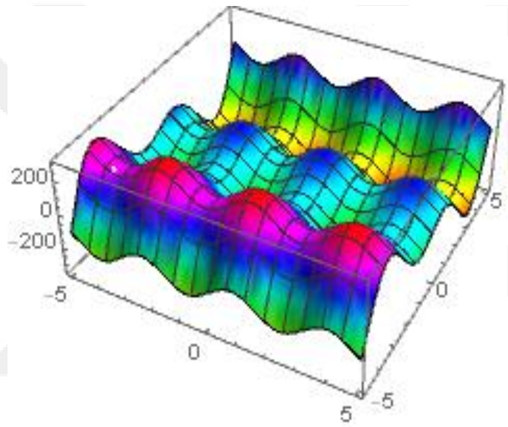

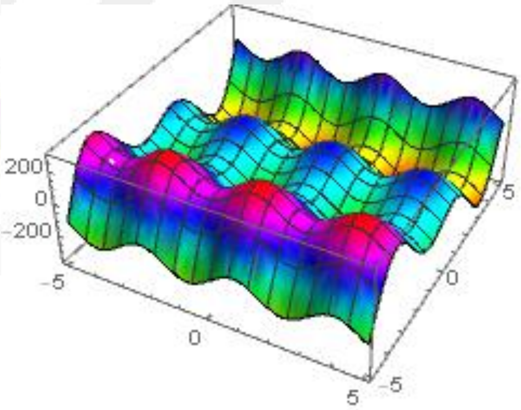

(e) exact solution at t=4 *(f) approximat solution at t=4*

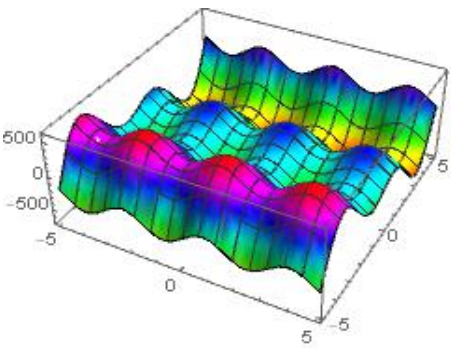

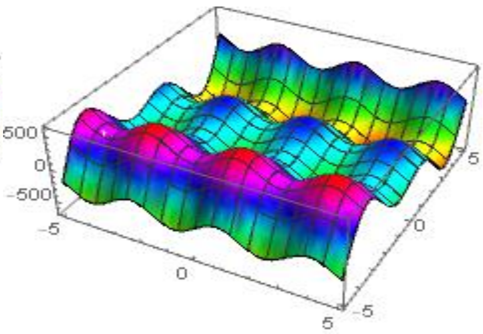

(g) exact solution at t=5 *(h) approximat solution at t=5*

Figure 4.3 (Continued) RMQ ($\lambda = 0.09$) is used in the area graphs of the numerical solutions at time $t = 2,3,4,5,6$ and 7 with $dx = 0.001$ and $dt = 0.0001$.

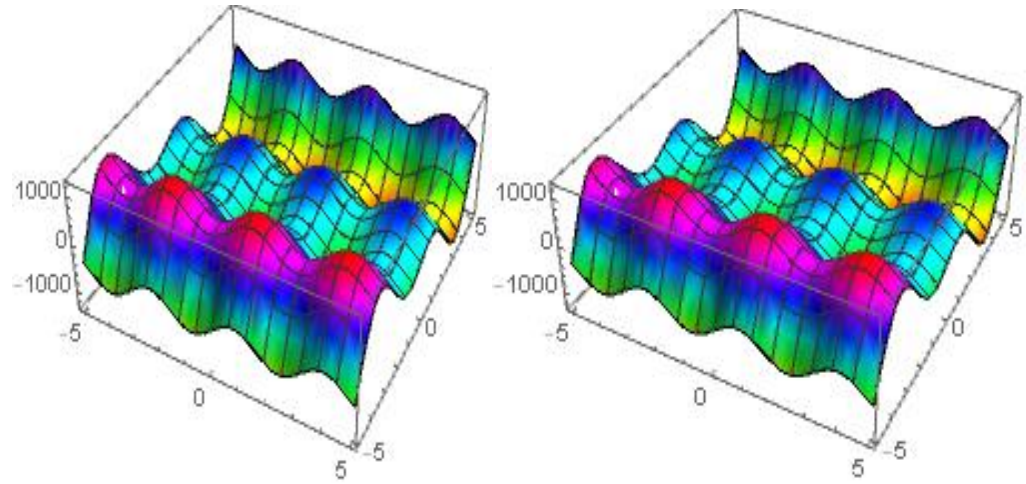

(i) exact solution at t=6 *(j) approximat solution at t=6*

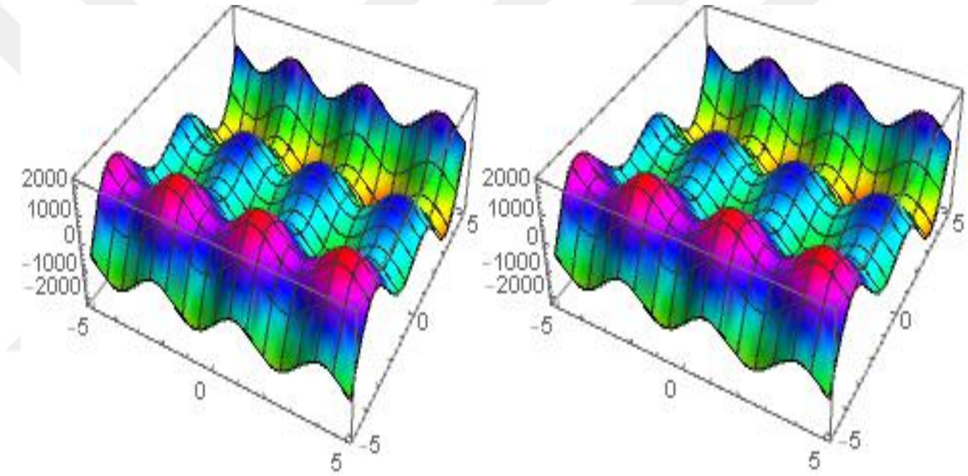

(k) exact solution at t=7 *(l) approximat solution at t=7*

Figure 4.3 (Continued) RMQ ($\lambda = 0.09$) is used in the area graphs of the numerical solutions at time $t = 2,3,4,5,6$ and 7 with $dx = 0.001$ and $dt = 0.0001$.

Application 4.4 Consider the following PDEs:

$$u_{ttt} + u_{tt} + u_t = u_{xx} + \pi u_x + g_2(x,t),\ 0 < x < 1, t > 0. \tag{4.10}$$

By comparing (4.10) with (3.3) then, $u_{tttt} = 0 = u_{xxx} = u_{xxxx}, \lambda = \mu = \nu = 1, \zeta = 0 = o = \eta = \upsilon, \sigma = 1, \kappa = \pi$, and; $g_2(x,t) = \cos(\pi x)$, with initial conditions

$$u(0,t) = 0,\ t > 0,$$

$u(1,t) = 0,\ t > 0,$

$u(2,t) = 0,\ t > 0,$

$u(3,t) = 0,\ t > 0,$

and

$$u(x,0) = \frac{\pi}{2} cos\ (\frac{\pi}{2}x),\ 0 \leq x \leq 1,$$

$$u_t(x,0) = \frac{\pi}{2} cos\ (\frac{\pi}{2}x),\ 0 \leq x \leq 1,$$

$$u_{tt}(x,0) = \frac{\pi}{2} cos\ (\frac{\pi}{2}x),\ 0 \leq x \leq 1 \tag{4.11}$$

$$u_{ttt}(x,0) = \frac{\pi}{2} cos\ (\frac{\pi}{2}x),\ 0 \leq x \leq 1.$$

The formula's analytical result of Equations (4.10), (4.11) is

$$(\frac{\pi}{2}t)\ u(x,\mathrm{t}) = \frac{\pi}{2} cos\ (\frac{\pi}{2}x) \tag{4.12}$$

The RMQ and SFS are employed to resolve this issue. For parameters $dx = 0.001$ and $dt = 0.0001$, following findings are obtained. For $t = 1,2,3,4,,5,6$ and 7, Table 4.7 lists the L_∞ , L_2, and RMS of Equation (4.12).

Table 4.7 Numerical errors using RMQ ($\lambda = 0.08$) and SFS ($m = 7$) represented at different times, where $dx = 0.001$ and $dt = 0.0001$.

T	L_∞		L_2	
	RMQ	**SFS**	**RMQ**	**SFS**
1	4.0287×10^{-5}	3.6266×10^{-5}	5.6354×10^{-4}	4.7534×10^{-4}
2	6.5243×10^{-4}	3.7350×10^{-4}	1.7647×10^{-5}	3.6629×10^{-5}
3	5.7622×10^{-4}	5.7655×10^{-5}	4.8252×10^{-6}	6.0834×10^{-6}
4	3.9265×10^{-6}	6.5286×10^{-6}	2.9927×10^{-5}	2.8801×10^{-5}
5	4.7624×10^{-5}	4.9254×10^{-5}	6.2651×10^{-5}	5.6277×10^{-5}
6	2.7530×10^{-6}	1.6538×10^{-6}	3.7538×10^{-5}	1.7543×10^{-5}
7	5.2755×10^{-6}	2.6588×10^{-5}	5.6443×10^{-6}	3.8150×10^{-6}

We also provide an RMQ assessment of a parameter estimate λ for outcomes. The L_∞ and L_2 errors using various λ at period $t = 7$ are displayed in Table 4.8.

Table 4.8 Numerical mistakes employing RMQ at time $t = 7$ where $dx = 0.001$, and $dt = 0.0001$ are expressed by a separate value λ

λ	$L\infty$	$L2$	RMQ
0.0	1.6438×10^{-6}	4.7542×10^{-6}	2.7051×10^{-6}
0.02	3.7524×10^{-6}	5.0329×10^{-5}	4.7432×10^{-4}
0.04	4.8275×10^{-5}	2.7533×10^{-5}	1.6430×10^{-5}
0.06	6.7542×10^{-5}	4.5661×10^{-4}	2.8543×10^{-4}
0.08	5.8632×10^{-4}	3.8242×10^{-4}	5.1892×10^{-4}

The space-time graphs of the numerical findings using RMQ ($\lambda = 0.09$) for $t = 2,3,4,6$ and 7 with $dx = 0.001$ and $dt = 0.0001$. The findings collected demonstrate the current approximation scheme's excellent precision and efficiency. It should be noted that in Figure 4.4, we are unable to tell the exact solution in addition to the approximated result.

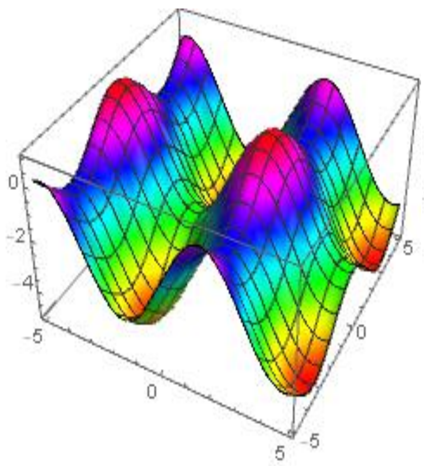

(a) exact solution at t=2

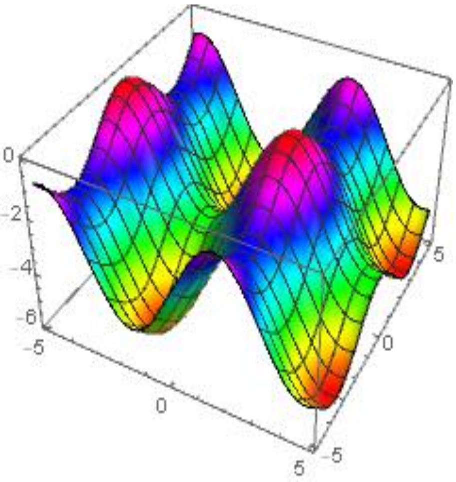

(b) approximat solution at t=2

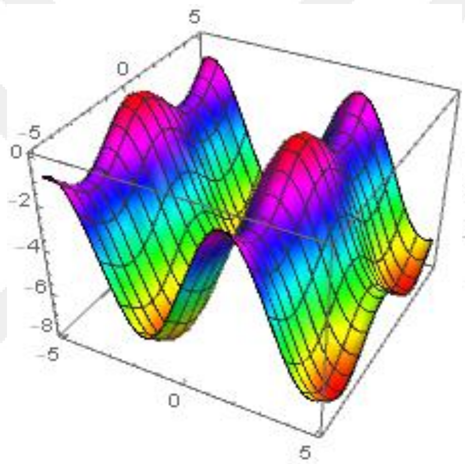

(c) exact solution at t=3

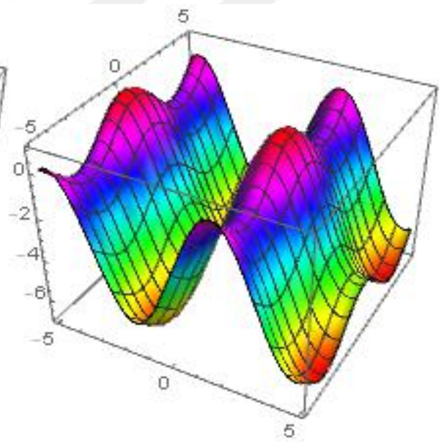

(d) approximat solution at t=3

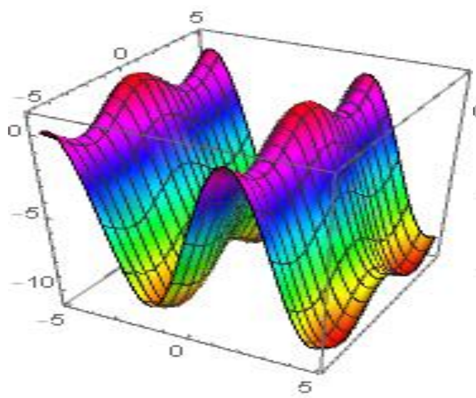

(e) exact solution at t=4

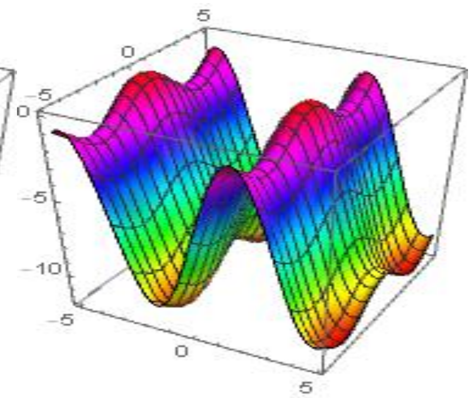

(f) approximat solution at t=4

Figure 4.4 RMQ ($\lambda = 0.09$) is used in the area graphs of the numerical solutions at time $t = 2,3,4,5,6$ and 7 with $dx = 0.001$ and $dt = 0.0001$

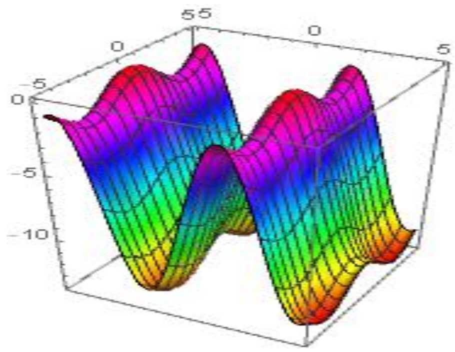

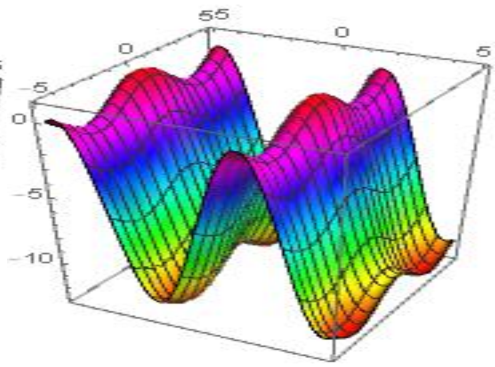

(g) exact solution at t=5 *(h) approximat solution at t=5*

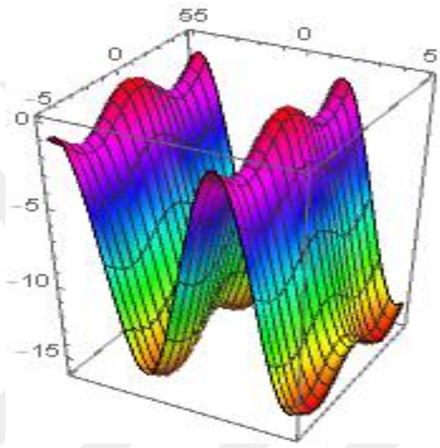

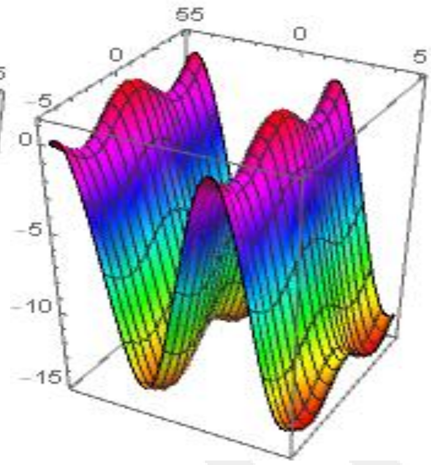

(i) exact solution at t=6 *(j) approximat solution at t=6*

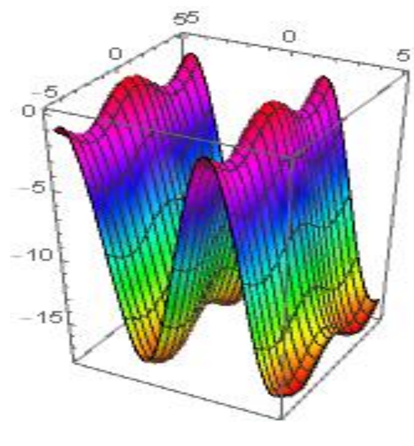

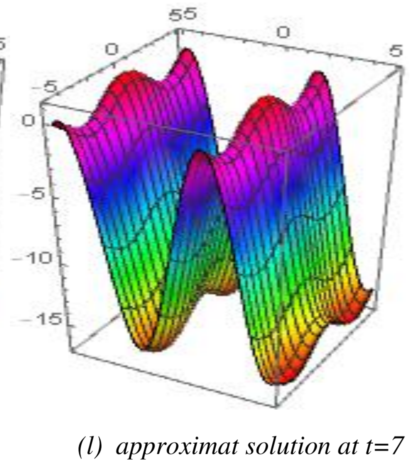

(k) exact solution at t=7 *(l) approximat solution at t=7*

Figure 4.4 (Continued) RMQ ($\lambda = 0.09$) is used in the area graphs of the numerical solutions at time $t = 2,3,4,5,6$ and 7 with $dx = 0.001$ and $dt = 0.0001$.

Application 4.5 Consider the following PDEs:

$$u_{ttt} + u_t = u_{xx} + 5u_x + g_2(x,t),\ 0 < x < 5, t > 0. \tag{4.13}$$

By comparing (4.13) with (3.3) then $u_{tttt} = 0 = u_{tt} = u_{xxx} = u_{xxxx}, \lambda = \mu = \nu = 1, \zeta = 0 = o = \eta = \upsilon, \sigma = 1, \kappa = 5$, and; $g_2(x,t) = \cos(\pi x)$ with initial conditions

$$u(0,t) = 0,\ t > 0,$$
$$u(1,t) = 5cos2t,\ t > 0,$$
$$u(3,t) = 2sin2t,\ t > 0,$$

and

$$\begin{aligned} &u(x,0) = cos3x,\ 0 \le x \le 5,\\ &u_t(\mathrm{x},0) = cos3x, t,\ 0 \le x \le 5,\\ &u_{ttt}(x,0) = -sin3x,,\ 0 \le x \le 5. \end{aligned} \tag{4.14}$$

The formula's analytical result of Equations (4.13), (4.14) is

$$u(x,\mathrm{t}) = cos\,(3x) sin(2t) \tag{4.15}$$

The RMQ and SFS are employed to resolve this issue. For parameters $dx = 0.001$ and $dt = 0.0001$, following findings are obtained. For $t = 1,2,3,4,5,6\ and\ 7$, Table 4.9 lists the L_∞ , L_2, and RMS of Equation (4.15).

Table 4.9 Numerical errors using RMQ ($\lambda = 0.09$) and SFS ($m = 7$) represented at different times, where $dx = 0.001$ and $dt = 0.0001$.

T	L_∞		L_2	
	RMQ	SFS	RMQ	SFS
1	4.7535×10^{-6}	6.7652×10^{-5}	4.1652×10^{-6}	2.7318×10^{-5}
2	7.2763×10^{-5}	3.1983×10^{-5}	6.3933×10^{-4}	4.6339×10^{-4}
3	6.3864×10^{-6}	2.8644×10^{-6}	1.0436×10^{-4}	5.8165×10^{-5}
4	3.2862×10^{-4}	5.0386×10^{-4}	3.9872×10^{-4}	2.9306×10^{-4}
5	1.3756×10^{-5}	6.3904×10^{-5}	5.2863×10^{-6}	3.7257×10^{-6}
6	7.2820×10^{-5}	3.8278×10^{-5}	2.8617×10^{-4}	1.7543×10^{-4}
7	3.9264×10^{-6}	5.2049×10^{-6}	7.2853×10^{-5}	6.2043×10^{-5}

We also provide an RMQ assessment of a parameter estimate λ for outcomes. The L_∞ and L_2 errors using various λ at period $t = 7$ are displayed in Table 4.10.

Table 4.10 Numerical mistakes employing RMQ at time $t = 7$ where $dx = 0.001$, and $dt = 0.0001$ are expressed by a separate value λ

λ	L_∞	L_2	RMQ
0.0	3.9620×10^{-7}	5.2802×10^{-7}	4.8244×10^{-7}
0.02	3.8257×10^{-6}	1.9927×10^{-6}	6.7306×10^{-5}
0.04	5.0278×10^{-6}	4.8736×10^{-5}	3.8155×10^{-5}
0.06	7.3861×10^{-5}	2.7396×10^{-5}	5.7534×10^{-5}
0.08	4.2769×10^{-4}	1.8653×10^{-4}	6.1154×10^{-4}

The space-time graphs of the numerical findings using RMQ ($\lambda = 0.09$) for $t = 2,3,4,6$ and 7 with $dx = 0.001$ and $dt = 0.0001$. The findings collected demonstrate the current approximation scheme's excellent precision and efficiency. It should be noted that in Figure 4.5, we are unable to tell the exact solution in addition to the approximated result.

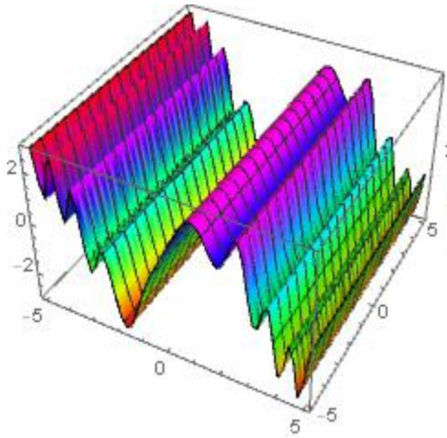

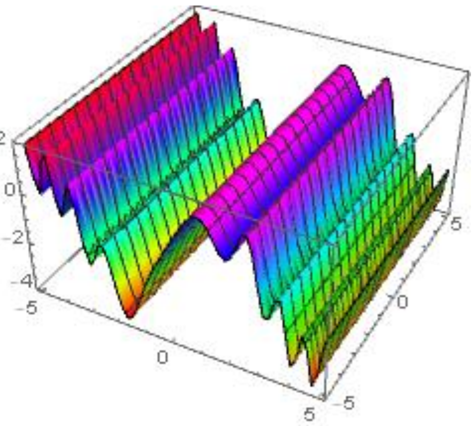

(a) exact solution at t=2 *(b) approximat solution at t=2*

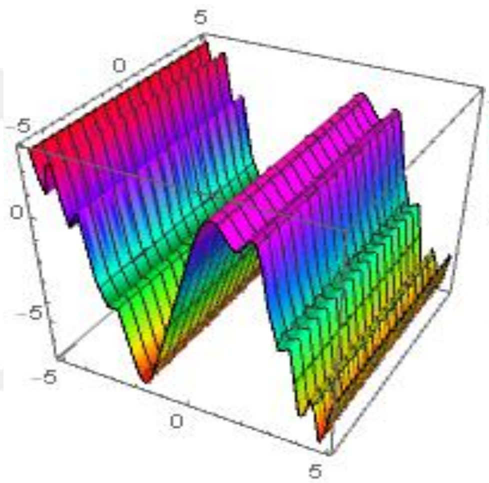

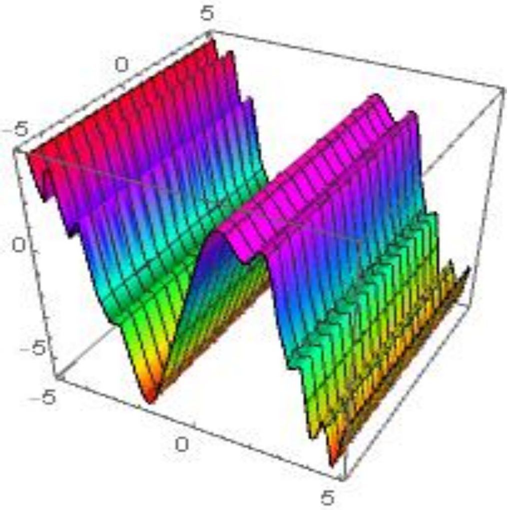

(c) exact solution at t=3 *(d) approximat solution at t=3*

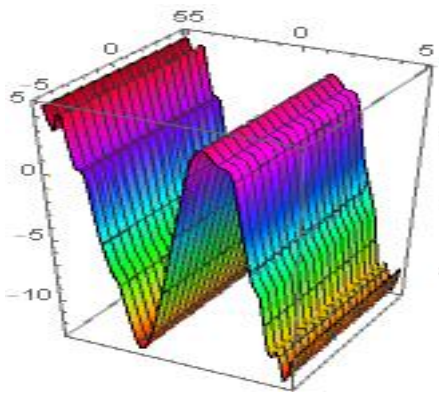

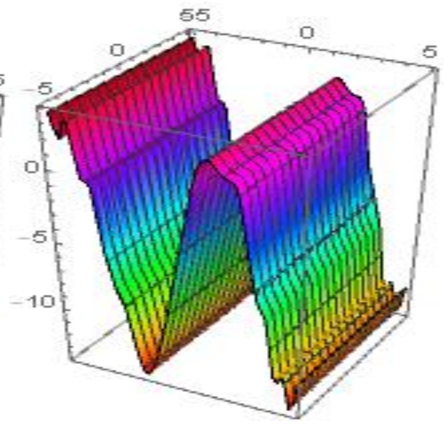

(e) exact solution at t=4 *(f) approximat solution at t=4*

Figure 4.5 RMQ ($\lambda = 0.09$) is used in the area graphs of the numerical solutions at time $t = 2,3,4,5,6$ and 7 with $dx = 0.001$ and $dt = 0.0001$

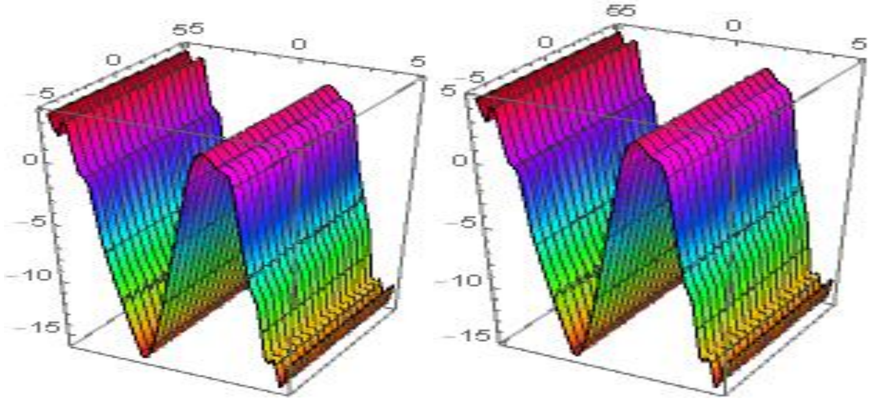

(g) exact solution at t=5 *(h) approximat solution at t=5*

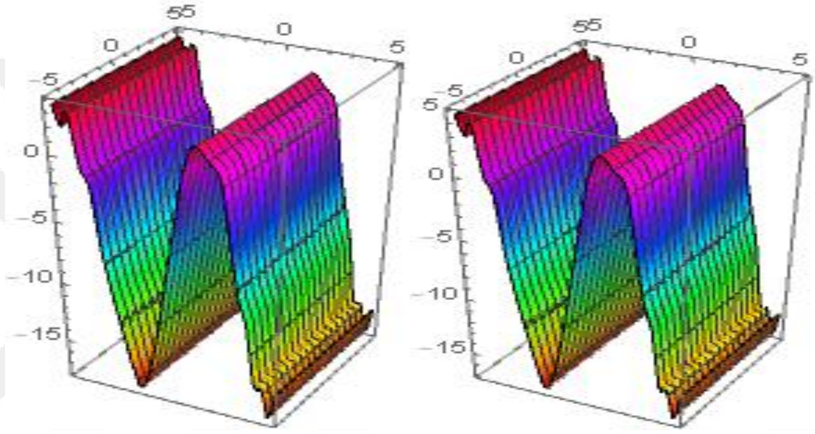

(i) exact solution at t=6 *(j) approximat solution at t=6*

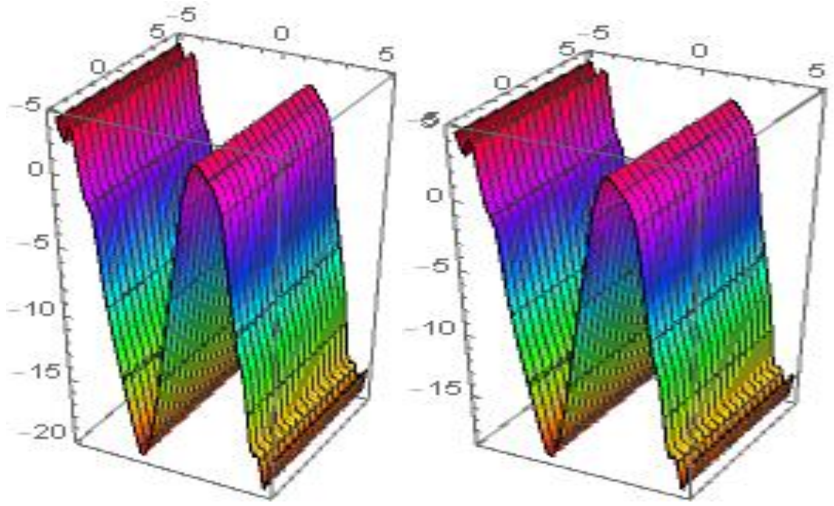

(k) exact solution at t=7 *(l) approximat solution at t=7*

Figure 4.5 (Continued) RMQ ($\lambda = 0.09$) is used in the area graphs of the numerical solutions at time $t = 2,3,4,5,6$ and 7 with $dx = 0.001$ and $dt = 0.0001$.

5. CONCLUSIONS AND RECOMMENDATION

5.1. Conclusions

The finite clouds approach is used to create a network analyzer of PDEs. To approximately solve the supplied PDE functions, this approach employs a construction methodology and a stable replication kernel. In this study, we offer a numerical technique for the network-free multi segmented and extended slender reverse radially functional network to solve time-dependent homogeneous issues. The primary benefit of this approach beyond finite - element approaches is that the former ones always offer a solution based on the grid elements. To show the reliability and viability of this strategy, five numerical examples are provided. The outcomes demonstrate the accuracy and perfection of our methodology. In reality, great numerical results can be achieved by choosing the right constant in the reverse voltmeter functions.

5.2. Recommendation

Numerous future study subjects have already been developed in view of an implementations and expansions for solving issues employing adaptable meshfree techniques. By utilizing the MFS with the adaptive technique, we can solve additional elliptical forms of PDEs in both 2D and 3D situations. As a result of our previous testing with various error estimation definitions, we can infer that additional error estimation kinds may be discovered and used to broaden the scope of the adaptable technique's use. It is possible to conduct more study on the mixing parameter and Neumann parameter issues with adaptive technique.

REFERENCES

Anitescu, C., Jia, Y., Zhang, Y. J. and Rabczuk, T. 2015. An isogeometric collocation method using superconvergent points. Computer Methods in Applied Mechanics and Engineering, 284: 1073-1097.

Atluri, S. N. and Shen, S. 2002. The meshless method. Encino: Tech Science Press.

Beel, A., Kim, T. Y., Jiang, W. and Song, J. H. 2019. Strong form-based meshfree collocation method for wind-driven ocean circulation. Computer Methods in Applied Mechanics and Engineering, 351: 404-421.

Belytschko, T., Lu, Y. Y. and Gu, L. 1994. Element-free Galerkin methods. International journal for numerical methods in engineering, 37(2): 229-256.

Bhrawy, A. H. and Baleanu, D. 2013. A spectral Legendre–Gauss–Lobatto collocation method for a space-fractional advection diffusion equations with variable coefficients. Reports on Mathematical Physics, 72(2): 219-233.

Boutayeb, A. and Chetouani, A. 2007. A mini-review of numerical methods for high-order problems. International Journal of Computer Mathematics, 84(4): 563-579.

Cahn, J. W., Elliott, C. M. and Novick-Cohen, A. 1996. The Cahn–Hilliard equation with a concentration dependent mobility: motion by minus the Laplacian of the mean curvature. European journal of applied mathematics, 7(3): 287-301.

Dehghan, M. 2005. Parameter determination in a partial differential equation from the overspecified data. Mathematical and computer modelling, 41(2-3):196-213.

Dehghan, M. 2006a. Implicit collocation technique for heat equation with non-classic initial condition. International Journal of Nonlinear Sciences and Numerical Simulation, 7(4): 461-466.

Dehghan, M. 2006b. Finite difference procedures for solving a problem arising in modeling and design of certain optoelectronic devices. Mathematics and Computers in Simulation, 71(1): 16-30.

Dehghan, M. and Shokri, A. 2008. A numerical method for solving the hyperbolic telegraph equation. Numerical Methods for Partial Differential Equations: An International Journal, 24(4):1080-1093.

Fasshauer, G. E. 2007. Meshfree approximation methods with Mattlb,Vol 6. World Scientific, 518 pages, London.

Ferreira, A. J., Kansa, E. J., Fasshauer, G. E. and Leitão, V. M. A. (Eds.). 2009. Progress on meshless methods. Dordrecht Springer, 291 page, Barcelona.

Griebel, M. 2005. Meshfree methods for partial differential equations II. M. A. Schweitzer (Ed.) Springer, 310 page, Berlin.

Jiang, T., Li, M. and Chen, C. S. 2012. The method of particular solutions for solving inverse problems of a nonhomogeneous convection-diffusion equation with variable coefficients. Numerical Heat Transfer, Part A: Applications, 61(5): 338-352.

Jiang, T., Jiang, Z. and Kolibal, J. 2013. A numerıcal method for 1d tıme-dependent schrödınger equatıon usıng radıal basıs functıons. International Journal of Computational Methods, 10(02): 1341010.

Kajishima, T. and Taira, K. 2016. Computational fluid dynamics: incompressible turbulent flows. Springer, 353 pages, Switzerland.

Kansa, E. J. 1990. Multiquadrics—A scattered data approximation scheme with applications to computational fluid-dynamics—II solutions to parabolic, hyperbolic and elliptic partial differential equations. Computers & mathematics with applications, 19(8-9): 147-161.

Li, M., Jiang, T. and Hon, Y. C. 2010. A meshless method based on RBFs method for nonhomogeneous backward heat conduction problem. Engineering Analysis with Boundary Elements, 34(9): 785-792.

Liu, G. R. and Liu, M. B. 2003. Smoothed particle hydrodynamics: a meshfree particle method. World scientific, 445 pages, London.

Liu, G. R. and Gu, Y. T. 2004. Boundary meshfree methods based on the boundary point interpolation methods. Engineering analysis with boundary elements, 28(5): 475-487.

Liu, G. R. and Gu, Y. T. 2005. An introduction to meshfree methods and their programming. Springer Science & Business Media, 473 page, New York.

Liu, G. R. 2009. Meshfree methods: moving beyond the finite element method. CRC press, 792 pages, Boca Raton.

Rabczuk, T. and Belytschko, T. 2004. Cracking particles: a simplified meshfree method for arbitrary evolving cracks. International journal for numerical methods in engineering, 61(13): 2316-2343.

Rabczuk, T., Belytschko, T. and Xiao, S. 2004. Stable particle methods based on Lagrangian kernels. Computer methods in applied mechanics and engineering, 193(12-14): 1035-1063.

Reddy, J. N. 2006. Theory and analysis of elastic plates and shells. CRC press, 568 page, London.

Schaback, R. 1995. Error estimates and condition numbers for radial basis function interpolation. Advances in Computational Mathematics, 3(3): 251-264.

Renardy, M. and Rogers, R. C. 2006. An introduction to partial differential equations Vol. 13. Springer Science & Business Media, 431 pages, New York.

Ren, R. F., Li, H. B., Jiang, W. and Song, M. Y. 2013. An efficient Chebyshev-tau method for solving the space fractional diffusion equations. Applied Mathematics and Computation, 224: 259-267.

Simo, J. C. and Hughes, T. J. R. 1985. Computational Inelasticity. Springer-Verlag, 389 pages, New York.

Smith, G. D. 1974. Numerical Solution of Partial Differential Equations. Oxford University Press, 334 pages, New York.

Smy, T., Walkey, D. and Dew, S. K. 2001. A 3D thermal simulation tool for integrated devices-Atar. IEEE Transactions on Computer-Aided Design of Integrated Circuits and Systems, 20(1):105-115.

Vlach, J., Jiří, V. and Singhal, K. 1983. Computer methods for circuit analysis and design. Springer Science and Business Media, 346 pages, Canada.

Wu, Z. M. and Schaback, R. 1993. Local error estimates for radial basis function interpolation of scattered data. IMA journal of Numerical Analysis, 13(1): 13-27.

Yoon, Y. C. and Song, J. H. 2014. Extended particle difference method for weak and strong discontinuity problems: part I. Derivation of the extended particle derivative approximation for the representation of weak and strong discontinuities. Computational Mechanics, 53(6): 1087-1103.

Zerroukat, M., Power, H. and Chen, C. 1998. A numerical method for heat transfer problems using collocation and radial basis functions. International Journal for numerical methods in Engineering, 42(7): 1263-1278.

CURRICULUM VITAE

Personal Information

Name and Surname : Mohammed Abdulrasool Hasan AL-DULAIMI

Education

MSc	Çankırı Karatekin University Graduate School of Natural and Applied Sciences Department of Mathematics	2021-2023
Undergraduate	Diyala University College of Science Department of Mathematics	2008-2009

Work Experience

An employee on permanent staffing at Diyala University for more than ten years.